

A SuperNEC Implementation of Model Based Parameter Estimation by Interpolating the Method of Moments Impedance Matrix

Neil Iain O'Leary

A dissertation submitted to the Faculty of Engineering and the Built Environment, University of the Witwatersrand, Johannesburg, in fulfilment of the requirement for the degree of Master of Science in Engineering.

Johannesburg, October 2006

Declaration

I declare that this dissertation is my own, unaided work. It is being submitted for the Degree of Master of Science in Engineering in the University of the Witwatersrand, Johannesburg. It has not been submitted before for any degree or examination in any other University.

Neil Iain O'Leary

This _____ day _____ of 2006

Abstract

SUPERNEC is a method of moments (MoM) electromagnetic field solver based on the Numerical Electromagnetics Code (NEC). Much of the simulation time can be attributed to the filling of the impedance matrix, which is performed at each frequency point of interest. Impedance matrix interpolation methods have been implemented in SUPERNEC to reduce the computational time required to fill the impedance matrix $[Z]$. Elements in $[Z]$ vary predictably over frequency and can be approximated by a second order polynomial. A second improved method is implemented where the dominant frequency variation term is removed prior to calculating the fitting function. A method of determining the optimum sample range relative to simulation range and maximum interaction distance has been developed. Given the correct choice of sample range the mean error in the MoM solution is less than 10% over the frequency range and the input impedance can be reproduced with good agreement over a wide bandwidth. Improvement in the simulation efficiency of 1.7 times can be expected if sufficient frequency points are of interest to account for the computational time required to sample the matrix and determine fitting function coefficients. This method has been applied to a dipole antenna, an LPDA and a horn antenna. To increase the simulation bandwidth and retain an acceptable level of accuracy, the bandwidth is split into multiple sub-bands.

Acknowledgements

I would like to thank Professor Alan Clark for his wisdom, guidance and comic relief

My parents for their support

Denel Aerospace for their financial support

Laura Manley, Dave Rice and Chris Barchievsky for helping me make valuable use of my spare time

Robert Hartleb for his help with C++ and L^AT_EX

Foreword

This dissertation is presented to the University of the Witwatersrand, Johannesburg for the degree of Master of Science in Engineering.

The dissertation is entitled “A SuperNEC Implementation of Model Based Parameter Estimation by Interpolating the Method of Moments Impedance Matrix”. The method increases the computational efficiency of the Method of Moments (MoM) by interpolating the Impedance matrix. The method was implemented using C++ in SuperNEC, a commercial electromagnetics simulation package. The code was extensively tested to find optimum sample range and solution error using Matlab. Radiation pattern interpolation methods were also explored.

This document complies with the university’s *paper model* format. The paper contains the main results of the research. The appendices present in detail the work conducted during the research.

Appendix A presents theory and method used to apply the impedance matrix interpolation to MoM and SuperNEC.

Appendix B presents the error analysis when the method is applied to a MoM structure. The method for determining the optimum sample range is discussed and applied to antenna structures.

Appendix C presents the analysis of the computational efficiency of the impedance matrix interpolation methods as compared to the standard SuperNEC computation.

Appendix D presents the interpolation of the SuperNEC radiation patterns with the use of rational functions.

Contents

| | |
|--------------------------|-------------|
| Abstract | ii |
| Acknowledgements | iii |
| Foreword | iv |
| Table of Contents | iv |
| List of Figures | vi |
| List of Tables | viii |

I Paper: A SuperNEC Implementation of Model Based Parameter Estimation by Interpolating the Method of Moments Impedance Matrix

| | | |
|-----|---|---|
| I | Introduction | 1 |
| II | Interpolation Method | 2 |
| III | Implementation for wire structures | 4 |
| | III-A Determining sample range | 4 |
| | III-B Required storage | 5 |
| IV | Results | 5 |
| | IV-A Dipole Antenna | 6 |
| | IV-B Log Periodic Dipole Array | 6 |
| | IV-C Horn Antenna | 7 |
| V | Improvement in computational efficiency | 7 |
| VI | Discussion | 7 |
| VII | Conclusion | 8 |
| | References | 8 |

II Appendices

| | |
|--|------------|
| A Theory and Method | A.1 |
| A.1 Introduction | A.2 |
| A.2 Model-Based Parameter estimation | A.2 |
| A.3 Method of Moments | A.2 |

| | | |
|----------|--|------------|
| A.3.1 | SuperNEC | A.4 |
| A.4 | Impedance matrix interpolation | A.4 |
| A.4.1 | Method of Least Squares | A.7 |
| A.4.2 | Windowing | A.7 |
| A.4.3 | Improved interpolation | A.9 |
| A.4.4 | <i>SuperNEC</i> implementation | A.10 |
| A.4.5 | Storage | A.12 |
| A.5 | Conclusion | A.13 |
| | References | A.16 |
| B | Error Analysis | B.1 |
| B.1 | Introduction | B.2 |
| B.2 | Error Analysis Method | B.2 |
| B.3 | Sampling | B.3 |
| B.4 | Confidence interval | B.6 |
| B.5 | Effect of specific simulation and structure properties | B.7 |
| B.5.1 | Error as a function of separation distance | B.7 |
| B.5.2 | Affect of problem size on solution accuracy | B.8 |
| B.5.3 | Error due to incorrect structure segmentation | B.8 |
| B.6 | Specific antenna cases | B.9 |
| B.6.1 | Dipole Antenna | B.9 |
| B.6.2 | Yagi antenna | B.11 |
| B.6.3 | Log periodic dipole array | B.12 |
| B.6.4 | Horn Antenna | B.14 |
| B.6.5 | UTD plate | B.15 |
| B.7 | Analysis of results | B.17 |
| B.8 | Conclusion | B.18 |
| | References | B.18 |
| C | Efficiency Analysis | C.1 |
| C.1 | Introduction | C.2 |
| C.2 | Simulation Time | C.2 |
| C.3 | Results | C.4 |
| C.4 | Conclusion | C.8 |
| | References | C.9 |
| D | Radiation Pattern Interpolation | D.1 |
| D.1 | Introduction | D.2 |
| D.2 | MoM far field calculation | D.2 |
| D.2.1 | Rational function overview | D.3 |
| D.2.2 | Implementation | D.3 |
| D.3 | Conclusion | D.5 |
| | References | D.6 |

List of Figures

| | | |
|------|--|------|
| 1 | Input impedance of 1m dipole antenna over wide frequency band | 3 |
| 2 | Three $[Z]$ elements over frequency | 4 |
| 3 | Three $[Z]'$ elements over frequency | 4 |
| 4 | $Z_{1,17}$ with polynomial approximation over wide frequency range | 5 |
| 5 | Graph relating the simulation range coefficient (k_f) to the sample range coefficient (k_f) | 6 |
| 6 | Graph relating the simulation range coefficient (k_f) to mean root square error over the simulation range | 6 |
| 7 | Root square structure current error over simulation range for dipole antenna | 7 |
| 8 | Input impedance of LPDA antenna via direct <i>SuperNEC</i> computation and Improved interpolation method | 7 |
| 9 | Root square structure current error over simulation range for LPDA antenna | 7 |
| 10 | Root square structure current error over simulation range for horn antenna | 8 |
| A.1 | Dipole antenna with 27 Segments | A.5 |
| A.2 | Input impedance of 1 metre dipole antenna | A.5 |
| A.3 | Real and Imaginary components of three impedance matrix elements over frequency | A.6 |
| A.4 | Error in impedance matrix when approximated by a 2^{nd} order polynomial vs sample range, for various number of samples used | A.6 |
| A.5 | Three overlapping Hann window functions | A.8 |
| A.6 | Impedance matrix elements approximated by piecewise windowed quadratic functions and a single quadratic function | A.8 |
| A.7 | Real and Imaginary component of three impedance matrix elements over a wide frequency band | A.9 |
| A.8 | Real and Imaginary component of three $[Z]'$ matrix elements over a wide frequency band | A.9 |
| A.9 | Flow diagram of improved interpolation scheme | A.11 |
| A.10 | Additional memory used in the impedance matrix MBPE methods | A.13 |
| B.1 | Sample range where minimum mean relative error occurs with increasing interaction distance | B.4 |
| B.2 | Simulation range coefficient (f_s) versus Sampling coefficient (k_s) for optimum sample range | B.5 |
| B.3 | Simulation range coefficient (f_s) versus average Root mean error over the simulation range | B.5 |
| B.4 | Mean relative current error and input impedance over frequency for Yagi antenna | B.6 |

| | | |
|------|--|------|
| B.5 | Mean relative current error and input impedance over frequency for Loop antenna | B.7 |
| B.6 | Relative error vs interaction distance of three segments structure | B.7 |
| B.7 | Graph showing average relative error for increasing number of structure unknowns | B.8 |
| B.8 | Input impedance of dipole antenna produced by <i>SuperNEC</i> with correct segmentation, incorrect segmentation and improved interpolation with incorrect segmentation | B.9 |
| B.9 | Input impedance of $0.5m$ dipole antenna via direct <i>SuperNEC</i> computation and MBPE methods | B.10 |
| B.10 | Root square structure current error over simulation range for dipole antenna | B.10 |
| B.11 | Input impedance of five element yagi antenna via direct <i>SuperNEC</i> computation and MBPE methods | B.11 |
| B.12 | Root square structure current error over simulation range for yagi antenna | B.12 |
| B.13 | Input impedance of LPDA antenna via direct <i>SuperNEC</i> computation and MBPE methods | B.13 |
| B.14 | Root square structure current error over simulation range for LPDA antenna | B.13 |
| B.15 | Elevation radiation pattern of LPDA at $380MHz$ and $600MHz$ | B.13 |
| B.16 | Input impedance of horn antenna via direct <i>SuperNEC</i> computation and MBPE methods | B.14 |
| B.17 | Root square structure current error over simulation range for horn antenna | B.15 |
| B.18 | Input impedance of Yagi antenna with UTD plate via direct <i>SuperNEC</i> computation and MBPE methods | B.16 |
| B.19 | Root square structure current error over simulation range for Yagi antenna with UTD plate | B.16 |
| B.20 | Input impedance and gain over dipole and dipole with electrically distant placed element | B.17 |
| | | |
| C.1 | MoM impedance matrix factor and solve time | C.3 |
| C.2 | Polynomial Coefficient Solve time | C.4 |
| C.3 | Impedance matrix fill time via polynomial interpolation | C.4 |
| C.4 | Mesh plot showing simulation time reduction (in seconds) for the impedance matrix interpolation schemes versus number of unknowns and simulation frequencies | C.6 |
| C.5 | 5 Element Yagi-Uda Antenna with wire grids | C.6 |
| | | |
| D.1 | Gain over frequency of a Yagi antenna with a Padé rational function fitting model | D.4 |
| D.2 | Yagi gain pattern as in <i>Figure D.1(a)</i> with and incorrect rational function order fitting model | D.4 |
| D.3 | Yagi Radiation pattern $90^\circ \leq \theta \leq 270^\circ$ with rational function interpolation | D.4 |

List of Tables

| | | |
|-----|--|------|
| I | Simulation time for antenna cases | 7 |
| A.1 | Guidelines for length and radius of individual segments | A.4 |
| A.2 | Guidelines for length and radius at segment junctions | A.4 |
| B.1 | Simulation parameters and results for dipole antenna | B.11 |
| B.2 | Simulation parameters and results for yagi antenna | B.12 |
| B.3 | Simulation parameters and results for LPDA antenna | B.14 |
| B.4 | Simulation parameters and results for horn antenna | B.15 |
| C.1 | Simulation time equation coefficients | C.5 |
| C.2 | Yagi - Uda structure simulation time | C.5 |
| C.3 | Patch antenna simulation time | C.7 |
| C.4 | Table showing simulation time for test cases with standard interpolation (MBPE ₁) | C.7 |
| C.5 | Table showing simulation time for test cases with improved interpolation (MBPE ₂) | C.7 |

Part I

Paper: A SuperNEC Implementation of Model Based Parameter Estimation by Interpolating the Method of Moments Impedance Matrix

A SuperNEC Implementation of Model Based Parameter Estimation by Interpolating the Method of Moments Impedance Matrix

Neil Iain O’Leary

Abstract—*SuperNEC* is a method of moments (MoM) electromagnetic field solver based on the Numerical Electromagnetics Code (NEC). Much of the simulation time can be attributed to the filling of the impedance matrix, which is performed at each frequency point of interest. Impedance matrix interpolation methods have been implemented in *SuperNEC* to reduce the computational time required to fill the impedance matrix $[Z]$. Elements in $[Z]$ vary predictably over frequency and can be approximated by a second order polynomial. A second improved method is implemented where the dominant frequency variation term is removed prior to calculating the fitting function. A method of determining the optimum sample range relative to simulation range and maximum interaction distance has been developed. Given the correct choice of sample range the mean error in the MoM solution is less than 10% over the frequency range and the input impedance can be reproduced with good agreement over a wide bandwidth. Improvement in the simulation efficiency of 1.7 times can be expected if sufficient frequency points are of interest to account for the computational time required to sample the matrix and determine fitting function coefficients. This method has been applied to a dipole antenna, an LPDA and a horn antenna. To increase the simulation bandwidth and retain an acceptable level of accuracy, the bandwidth is split into multiple sub-bands.

Index Terms—MoM efficiency, Impedance matrix interpolation, *SuperNEC*

I. INTRODUCTION

THE use of the Method of Moments (MoM) as a frequency domain field solver is a well used technique to accurately predict the electromagnetic (EM) characteristics of large structures [1]. When designing antennas, observable parameters such as input impedance, VSWR and radiation patterns are required over a wide frequency range [2]. Generation of wide bandwidth EM information using MoM is a computationally expensive task as the MoM procedure is performed at each frequency point of interest. Much of the computational time used is in the filling and solving of the $N \times N$ impedance matrix ($[Z]$), where N is the number of unknowns in the problem.

Miller in [3] introduced Model-Based Parameter Estimation (MBPE) as a form of “smart” curve fitting. Where a fitting model (FM) is applied to a observable parameters itself [4] or in the formulation field solver [5] thus reducing the computational time in generating the wide bandwidth information with minimal loss in solution accuracy. MBPE was applied in [6] to increase the computational efficiency of determining EM transfer function with the use of a rational

function which is solved using the Padé procedure [7].

MBPE was applied to the efficient generation of radiation patterns by Werner in [8] spatially and over the frequency. This method uses the Padé rational function to approximate the radiation pattern. The rational function coefficients are determined by sampling far electric field values at various spacial and frequency points. This method was implemented by the author in *SuperNEC* in [9] with poor results. Correct rational function order is critical in obtaining an accurate fitting model, this requires *a priori* knowledge of the number of poles in the transfer function.

Werner further improved this method in [10] to fixed order rational function over smaller sub-bands. The method can however be used to reduce the amount of storage required in storing wideband three dimensional radiation patterns as the FM can be stored instead of all the numerical values.

Each of the impedance matrix elements is determined by evaluating a integral over the segment length [11]. While simple numerical integration techniques have been developed [12] these integrals are evaluated for each source-observation point in the structure at every observation frequency. Computational efficiency can be improved if the evaluation of the integral is replaced with a simple FM model. Impedance matrix interpolation as a form of MBPE was implemented by Newman [13] where the impedance matrix elements were approximated by simpler quadratic fitting functions thus reducing the time required to fill the impedance matrix. Newman applied the method to dipole antenna cases producing accurate approximations. The method was further applied to mobile communication antennas by Rahmat-Samii [14], a method of interpolating the admittance matrix ($[Y]$) with rational functions was also implemented in this paper thus removing the need to invert the impedance matrix. A high order rational function was needed to accurately approximate the unpredictable admittance matrix elements and with improved matrix inversions methods such as LU decomposition [15] make the efficiency improvement in this method negligible. The method has been applied to planar microstrip antennas in [16], [17] with accurate results and good improvements in computational efficiency.

SuperNEC is an object-oriented (OO) C++ [18] implementation of the MoM Numerical Electromagnetics Code (NEC2) originally developed by the Lawrence Livermore Laboratory

[11]. The OO nature of the code makes it possible to easily add functionality to the code, additions include a Uniform Geometric Theory of Diffraction (UTD) MoM hybrid [19], dielectric coated wires and a MoM parallel implementation [20].

Impedance matrix interpolation methods have been implemented in the *SuperNEC* code, this is achieved by approximating the elements in the impedance matrix with a quadratic function. Two methods have been implemented: a standard method where all the elements are approximated with a quadratic function directly, and improved method where the frequency variant component is removed prior to approximation and a windowed sub band method. A detailed explanation of the theory and implementation of these methods can be found in [21]. Section II outlines the MoM procedure and impedance matrix interpolation method, Section III is on how the method was implemented in *SuperNEC* and determining correct sample range. Results applied to antenna cases and computational efficiency of the methods are discussed in Section IV and Section V respectively.

II. INTERPOLATION METHOD

The Electric Field Integral Equation (EFIE) is solved in MoM by splitting the structure into N short thin pieces or segments such that the thin wire approximation [11] can be applied. The currents on each of the segments are solved by a linear system in Eq. (1) where $[Z]$ is the generalised impedance matrix, $[I]$ is the unknown structure current vector and $[V]$ is the known excitation.

$$[Z][I] = [V] \quad (1)$$

The impedance matrix is can be referred to the as matrix of mutual impedance between source segments m and observation segment n , notation used to refer to a single entry in the matrix is $Z_{m,n}$. Each element in $[Z]$ is determined by:

$$Z_{m,n} = \int_L f(s) \left[\frac{\delta^2}{\delta s \delta s'} g(r_m, r_n) + k^2 g(r_m, r_n) \right] ds' \quad (2)$$

$$\text{Where } g(r_m, r_n) = \frac{e^{-jk|\vec{r}_m - \vec{r}_n|}}{|\vec{r}_m - \vec{r}_n|}$$

is the free space Green's function and $f(s)$ is a set of sine, cosine and constant basis functions used the MoM procedure [11].

Much of the computational time in MoM is in the filling of the $N \times N$ impedance matrix $[Z]$ which is performed at every frequency point of interest. If the matrix filling function in Eq. (2) can be replaced with a simple FM the computational time used to fill $[Z]$ can be greatly reduced. Approximating the MoM solution $[I]$ is difficult due to the unpredictability of the frequency variation, a high order rational function is needed to for an accurate FM.

The elements in the impedance matrix vary predictably over frequency, hence it is possible to approximate the elements in the matrix with a low order polynomial function or Taylor series. Consider a 1 Metre long dipole antenna segmented in 30 equal pieces, the input impedance of the antenna over a wide frequency range, 100MHz to 800MHz, is shown in Fig. 1. By

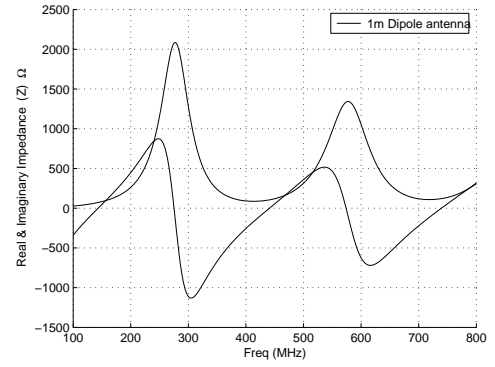


Fig. 1. Input impedance of 1m dipole antenna over wide frequency band

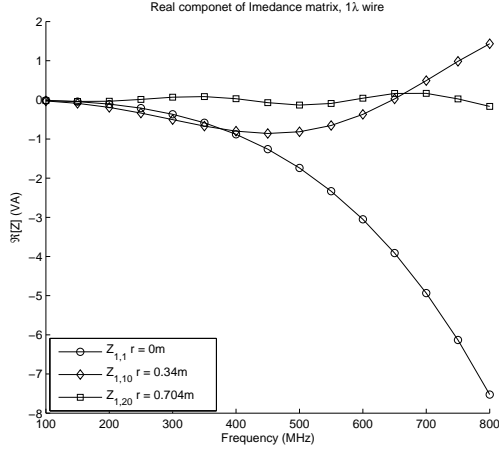
contrast consider three element of the impedance matrix in Fig. 2: $Z_{1,1}$ represents the self impedance of the first segment, $Z_{1,10}$ is the mutual impedance between the first and tenth segment (0.34m apart) and $Z_{1,20}$ is the mutual impedance between the first and twentieth segment (0.7m apart). While the frequency variation increases with the interaction distance it is still significantly less than is the case of the input impedance. The input impedance could be easily approximated with the use of a rational impedance given the correct order for this case, however for an antenna with a greater level of variation in the observable the FM order would not hold. Variation in impedance matrix elements is constant for any given antenna characteristics, this factor makes it possible to apply MBPE to accurately approximate the observables for a generalised structure. Interpolation the elements in the impedance matrix directly over frequency is known as the standard interpolation method.

From Eq. (2) it is clear that frequency variation term $e^{-j2\pi\lambda\vec{R}}$, where \vec{R} is the interaction distance between the source and observations segments, begins to dominate as the interaction distance increases. For interaction distances greater than 0.5λ removing this terms results in the impedance matrix elements becoming more predictable over frequency. Thus a new matrix is $[Z]'$ generated by:

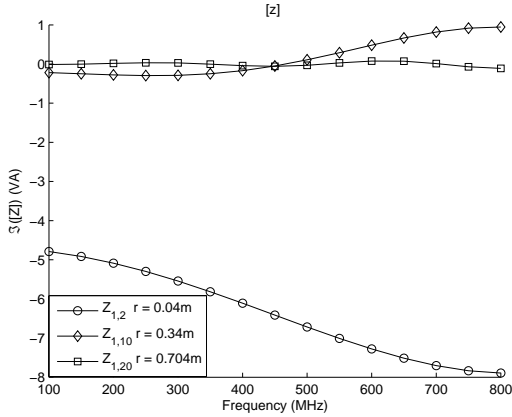
$$[Z]' = \frac{[Z]}{e^{-j2\pi\lambda\vec{R}}} \quad (3)$$

Fig. 3 shows the same impedance matrix elements as Fig. 2 with the variant component removed. It is clear that the frequency variation is significantly less and a simple approximation model could be used to accurately approximate the elements over a wide frequency bandwidth. Fitting a second order polynomial function to the $[Z]'$ matrix is referred to as the improved interpolation method. The improvement in simulation efficiency is not as great as the standard method explained above as computational effort is required to remove the variant components after sampling and reintroducing it when filling the matrix by evaluating the quadratic functions.

Coefficients of the fitting function are determined by sampling the matrix at specified frequency points, this is achieved by filling the matrix in the standard fashion for the standard interpolation method. Samples for the improved method have the variant component removed before the coefficients are



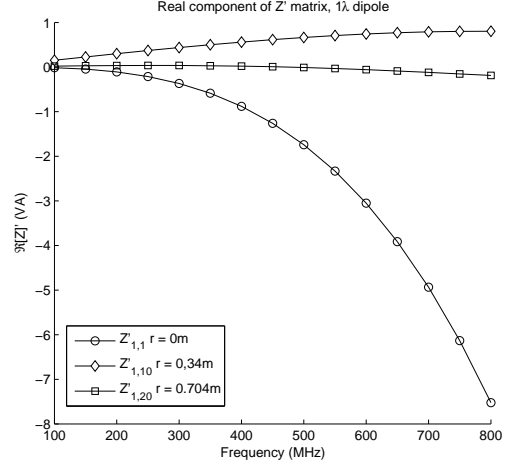
(a) Real Components



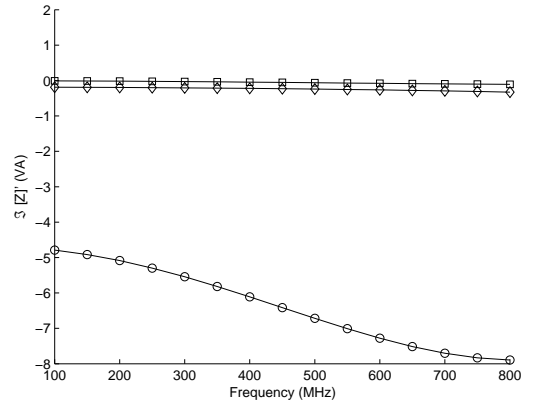
(b) Imaginary Components

Fig. 2. Three $[Z]$ elements over frequency

solved. As the elements in the impedance matrix are complex two fitting functions are required to approximate each of the elements. Newman used a quadratic function to approximate the real components and a logarithmic expression to account for the logarithmic singularity with frequency of element self impedance [13]. However it was found that a quadratic function could approximate the imaginary component as well without the need for introducing logarithmic functions. The method of least squares was used to determine the coefficients of the polynomial fitting functions as the method is flexible as to polynomial order and number of samples used to determine the coefficients [23]. A better approximation was expected when using a higher order polynomial approximation or when sampling a higher number of sample points. In testing with various polynomial orders and sample frequencies it was found that the sample range (Δf) of the sample points had the greatest effect on the accuracy in the solution [21]. The error level converges when the optimum sample range is used, the method of determining this range is covered in Section III.



(a) Real Components



(b) Imaginary Components

Fig. 3. Three $[Z]'$ elements over frequency

Fig. 4 shows a second order polynomial function approximating $Z_{1,17}$ for a wire structure, the separation distance of the two elements is 0.5m. The standard interpolation method holds over a small frequency range but becomes highly inaccurate toward the upper end of the range. By contrast the improved interpolation method shows an accurate approximation of the element over the entire frequency range. While these figures show that the standard method is highly inaccurate the method should not be discounted for electrically small structures and small frequency bandwidths due to the superior efficiency increase compared with the improved method.

III. IMPLEMENTATION FOR WIRE STRUCTURES

Wire structures in *SuperNEC* are modelled by interconnected segments and plates as mesh segments grids [24]. It is of utmost importance that the structure is segmented correctly. Restrictions in the segments length, radius and interconnection are due to the assumptions in reducing the EFIE from a vector

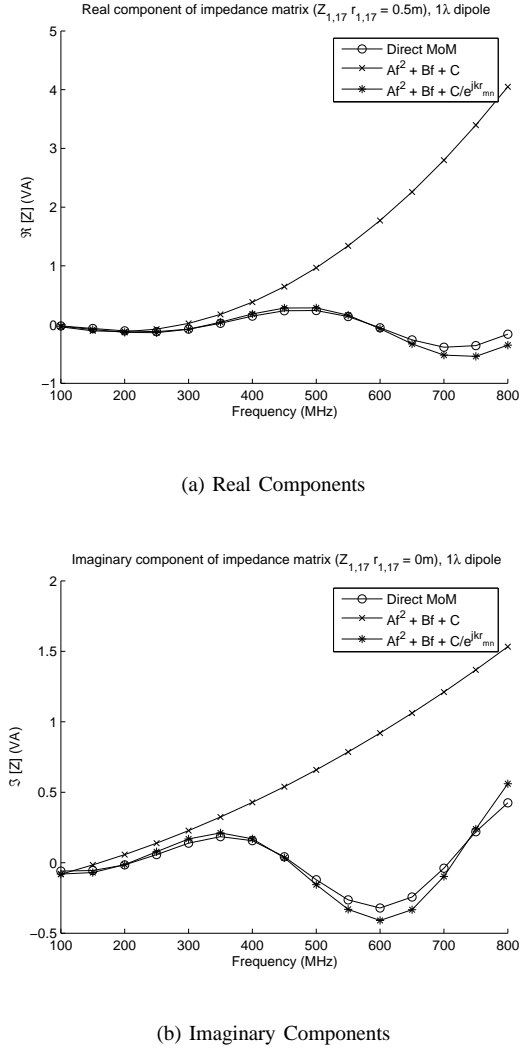


Fig. 4. $Z_{1,17}$ with polynomial approximation over wide frequency range

to a scalar equation, the restrictions themselves can be found in [25]. An incorrectly segmented structure will result in errors in $[Z]$ and ultimately the MoM solution. When approximating $[Z]$ elements the error is compounded as they no longer follow a non-pole relationship over frequency. Neither the standard nor improved methods of approximating the elements can be used. When using impedance matrix interpolation the structure should be segmented at the highest frequency of interest. A higher segmentation frequency will result in a shorter segments and hence more unknowns in the solution. A trade off between accuracy in the MBPE solution and simulation efficiency results as segmentation at a lower frequency may produce less accurate results but a greater simulation speedup will be achieved. Where possible frequency scaling should be used to reduce the problem size and the minimum possible upper frequency should be used for segmentation. Another method to counteract the segmentation paradox is to use multiple sub-bands, where the simulation frequency range is split into smaller bands with impedance matrix interpolation performed on each of the smaller bands. Each sub-band

upper frequency should be used for the segmentation of the structure thus reducing the problem size for the all but the upper most frequency band. Discontinuities will result between band junctions, a trade off which may be acceptable given a sufficient speedup in simulation time. Discontinuities can be minimised by using overlapping bands with a window function to smooth the junction, as was implemented by the Author with impedance matrix elements in [21].

A. Determining sample range

Interaction distance between source and observations segments has the greatest effect on the variation of the elements in the impedance matrix, while the elements in the reduce variation matrix are as dependent on interaction distance the effect is still apparent.

MoM solution accuracy depends on choice of correct sample and simulation range. The method used by Newman in [13] was to apply the Nyquist sampling criteria such that wavenumber step (Δk) size is less than π . Maximum sample range can thus determined by:

$$\Delta f_s = \frac{f}{2R_\lambda^{\max}} \quad (4)$$

This specifies the upper step size for the standard interpolation method and as a result a smaller step size should be used when applying standard interpolation and a greater one for the improved method. This method does not however specify the bandwidth over which the interpolation function can be accurately extrapolated. Eq. (4) also only relates the sample range to the maximum interaction distance of the structure and not the simulation range. If a narrow frequency band is required it would be advantageous to sample over a narrower band than specified by Eq. 4. Yeo and Mittra in [16] related the sample range to the upper frequency value by specifying f in Eq. (4) to be the upper most frequency value of interest (f_{\max}). Given an upper frequency value too high this method would produce inaccurate results as the fitting functions would be poorly conditioned. For structures with a maximum interaction distance of less than 1λ a too wide sample range would be achieved, again resulting in poorly conditioned fitting functions. Segmentation must be done at the highest frequency of interest whether it be a sample or simulation frequency, thus there is no point in sampling at higher frequencies than are of interest.

The sample range from Eq. (4) is reduced by the addition sample range coefficient (k_s):

$$\Delta f_s = k_s \times \frac{f_{\text{centre}}}{2R_\lambda^{\max}} \quad (5)$$

(k_s) is determined by the total simulation range (f_M) in order to minimise the error for specified simulation range and maximum interaction distance. The simulation range is specified as an input parameter and related to the maximum interaction distance by a simulation range coefficient (k_f):

$$f_M = k_f \times \frac{f_{\text{centre}}}{R_\lambda^{\max}} \quad (6)$$

In general it was found that if the required simulation range coefficient (k_f) was greater than one the simulation band is too large and should be split into sub-bands. As mentioned before if the maximum interaction distance is less than 1λ unity should be used for the maximum interaction distance. The curves in Fig. 5 are used to obtain (k_f) from the simulation range coefficient calculated in Eq. (6). These curves were produced by simulation an arbitrary wire structure over the simulation ranges varying the sample range, the point where minimum error was achieved was noted. This process was repeated for increasing interaction distance case, the number of unknowns in the structure were kept constant as increasing the problem size would change the level of error achieved. Fig. 5 is for the improved interpolation case, the curve for the standard interpolation although similar can be found in [26]. Mean square structure current error over the entire simulation range was used to calculate the error in the simulation, the method will be discussed in greater depth in Section IV.

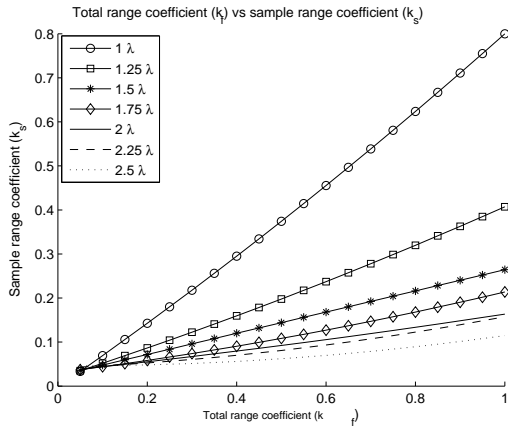


Fig. 5. Graph relating the simulation range coefficient (k_f) to the sample range coefficient (k_s)

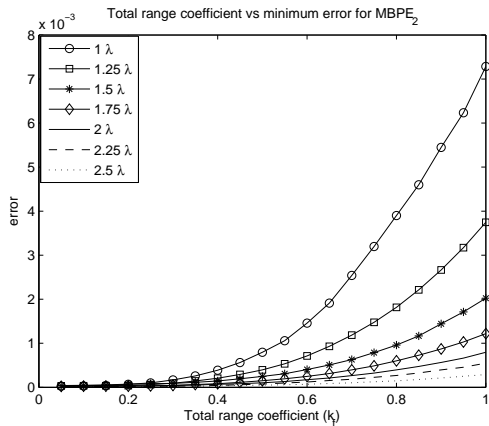


Fig. 6. Graph relating the simulation range coefficient (k_f) to mean root square error over the simulation range

Fig. 6 shows the mean root square error over simulation range coefficient (k_f) for increasing maximum interaction distance. The error in the solution steadily increases with increasing simulation range and given a too large simulation

range the error in the solution becomes unacceptable. Note that the above curves must only be used as a guide as to the error in the solution. Other factors such as the number of segments in the structure, position of all the segments and segment connection will effect the final accuracy of the solution.

B. Required storage

The amount of additional memory used in the MBPE scheme is worth noting. Since three impedance matrices must be filled and stored in order to calculate fitting function coefficients the amount of additional memory increases rapidly with problem size. Another source of additional memory required is in the storing of the fitting function coefficients themselves, three coefficients are required for the fitting function. Impedance matrix elements and fitting function coefficients are complex values each expressed by two *float* value, the amount of additional memory in bytes is:

$$\text{MEM}_{\text{max}} = (8 \times 7.5)N^2 \quad (7)$$

This is for the improved interpolation case, where three samples are taken for second order polynomial fitting function. As the problem size exceeds 800 unknowns 1GB of additional memory is required.

IV. RESULTS

The usefulness of any optimisation method is determined by how accurately it can be used and the improvement in efficiency. When using approximation functions as is the case with impedance matrix interpolation a certain level of accuracy will be lost, in general this error will increase with extrapolation past the centre frequency. One of impedance matrix interpolation's best attributes is it's the ability to apply the technique to any structure. The method has been applied to various wire and grid structures, these are a Dipole antenna, Log periodic dipole array and a horn antenna. Each of these introduce different elements in the simulation, being size, make up of structure and addition of transmission lines. In order to specify error it is important to have an error norm, which must be applied to a element of the simulation being either in the simulation domain or the solution domain. Looking at the error of the impedance matrix approximation functions is not useful as error in the impedance matrix will be increased when the matrix is inverted and solution found. On the other hand looking at an observable parameter such as input impedance will also not give a realistic error norm as input impedance is only calculated on a single segment (as is the case when a single excitation is used). Error in segments far away from the excitation would not have a great effect the input impedance however would have a significant effect on the radiation pattern. Error in radiation pattern is a good method as it incorporates all the effect of all the segments, radiation pattern specified in dB gives a intuitive value for error. Calculation of wideband three dimensional radiation patterns however is not only computationally expensive a large amount of storage is needed to post process the results. The error norm is thus calculated with the MoM solution, the current vector $[I]$. Relative root mean square error is used as it gives the most

intuitive results and offsets in phase do not cause an unrealistic amount of solution error. The error as a function of frequency is defined by:

$$e(f) = \frac{1}{N} \sqrt{\sum_{k=1}^N \frac{|I_k - I_k^m|^2}{|I_k|^2}} \quad (8)$$

A norm as the mean error over the frequency range is then:

$$\|e\| = \frac{1}{n_f} \sum_{f=1}^{n_f} e(f) \quad (9)$$

A confidence interval is defined as the frequency range extending on either side of the centre frequency where the error is less than 10%. It is often found that the confidence interval is greater on the upper frequency range than the lower however is expressed by a single value. The confidence interval gives a user an idea of the simulation range that the technique can be used and still reproduce accurate results.

A. Dipole Antenna

The impedance matrix interpolation technique was applied to a 0.5m dipole antenna with a centre frequency of 500MHz. The dipole antenna is used as it's simplicity in structure and in observables [2] makes it good for benchmarking the technique. In general MBPE techniques would not be applied to cases this small and simple as simulation from first principles can be done quickly with modern computers.

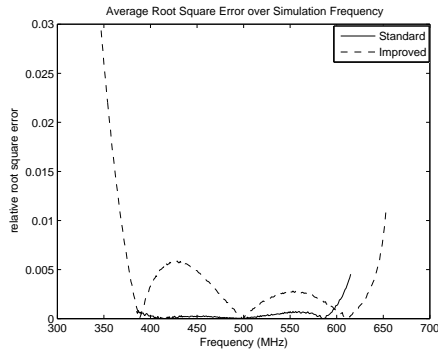


Fig. 7. Root square structure current error over simulation range for dipole antenna

Fig. 7 shows the mean root square error over frequency for the dipole antenna, both method show a low level of error over the entire range being 0.04% and 0.4% for the standard and improved methods respectively. In cases such as this where the maximum interaction distance is small the standard method outperforms the improved one. While the error is small for both case the simulation time improvement is better of the standard case being 36% apposed to 34% with improved method. However the gain in seconds is so slight that the loss in accuracy is not worth the speedup in simulation time.

B. Log Periodic Dipole Array

Broadband antennas such as the LPDA are ideally suited to MBPE method due to the wide frequency range required and size of the structure [27]. As there are many variable parameters in the structure numerous computer simulations are required to optimise the design. Even a small increase in simulation efficiency will result in a large time reduction when computing observables for a large number of cases. The LPDA brings transmission lines into the structure which effect the performance if the impedance matrix fitting models.

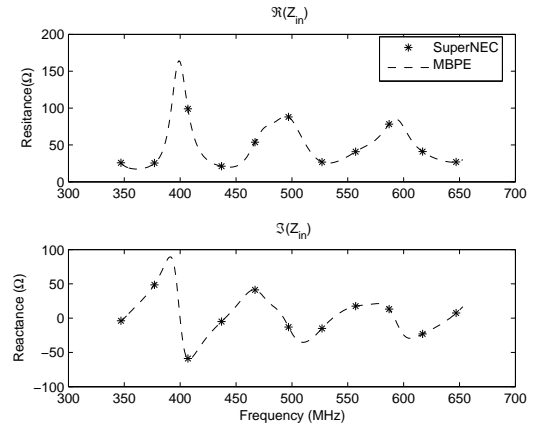


Fig. 8. Input impedance of LPDA antenna via direct *SuperNEC* computation and Improved interpolation method

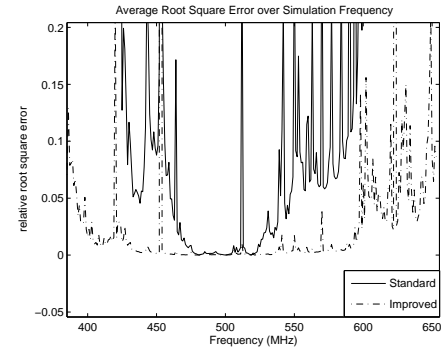


Fig. 9. Root square structure current error over simulation range for LPDA antenna

Fig. 8 shows the input impedance the LPDA antenna and the impedance generated with the improved interpolation method. The observable curve is well conditioned over the entire range. Consider the root square error in Fig. 9, the standard method shows a high level of inaccuracy while the improved method has acceptable error over the simulation range. Sparse points of increased error are attributed to the transmission line in the solution, further work is needed to generate a fitting model to account for the elements. However the a mean error of 2.8 % can be expected in the confidence interval of 147 MHz with a simulation time speedup of 41%. The radiation pattern is also well reproduced when using the improved method, the radiation pattern can be found in [26].

C. Horn Antenna

Like the LPDA horn antennas are used in broad-band applications, they consist of a waveguide element connected to a conical or pyramid radiation element [28]. Metal plates are modelled as grid mesh of wire segments, a large number of segments are required modelling such plates. Simulation time is further increased in NEC as the number of junctions at the segment ends is greater than wires. The basis functions are evaluated over all the adjacent connected segments [11], however when filling the matrix from the fitting model only a single calculation is needed for each element independent of connection. To increase the simulation bandwidth this total simulation bandwidth was split into two sub-bands the first extending from 207-390 MHz with a center frequency of 400 MHz and a second extending from 395-500 MHz with a center frequency of 450MHz. To reduce the problem size the first band was segmented at 300MHz and the second at 500MHz resulting in a problem size of 1289 and 3535 unknowns respectively. Only the improved interpolation method was used for this example as the maximum interaction distance was 2.2 metres.

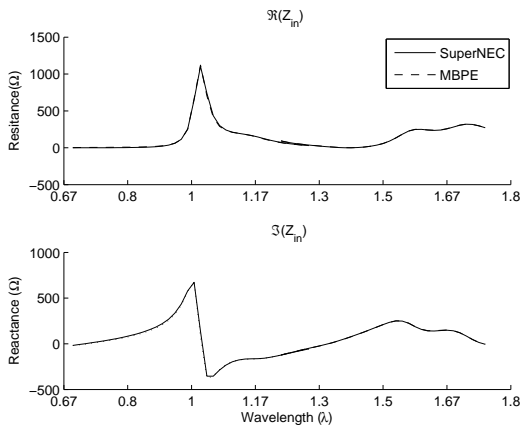


Fig. 10. Root square structure current error over simulation range for horn antenna

Fig. 10 show the input impedance of the antenna over both the frequency bands, the impedance matrix interpolation method reproduces the curve well over the entire frequency band. There is a discontinuity between bands however it is the same for the *SuperNEC* and MBPE cases, this is due to the different segmentation frequencies. Mean root square error for the first band is 18.9% and the second 19.8%. This level of error is higher than in previous examples due to the large number of segments in the structure and large interaction distances. The error however in the input impedance is relatively small in comparison due to the reduced effect the elements with large interaction distances have on the input impedance.

V. IMPROVEMENT IN COMPUTATIONAL EFFICIENCY

The computational time required to in the MoM is proportional to $N^2 f$ [29] where N is the problem size and f the number of frequency values of interest. Whether the impedance matrix elements are calculated from direct computation or by evaluating a fitting function the simulation

time will be proportional to this factor. Additional time which must be made up when using impedance matrix interpolation is in the sampling of the impedance matrices and solving fitting function coefficients. A break even point can be found, for small problems (less than 500 unknowns) 17 and 38 frequency points must be of interest for the standard and improved method respectively in order to obtain an increase in efficiency [30]. This is a guide a matrix filling time differs for different structure geometries. Solving of the matrix is performed with LU decomposition: an N^3 process [31], this term is expected to dominate simulation time are the problem size increases sufficiently. However problems sizes exceeding 5000 unknowns have been tested with the dominant time component remaining the matrix filling time.

Impedance matrix interpolation was applied to various wire and grid antenna structures, the simulation time performance is shown in Table I

TABLE I
SIMULATION TIME FOR ANTENNA CASES

| Antenna | N | f | [Z] fill time | | Time Gain | |
|---------|------|-----|---------------|-------|-------------|-------|
| | | | Direct | MBPE | Direct/MBPE | (s) |
| Dipole | 15 | 307 | 0.016 | 0.01 | 1.71 | 1.23 |
| Yagi | 50 | 290 | 0.047 | 0.031 | 2.16 | 6.85 |
| LPDA | 221 | 240 | 0.568 | 0.454 | 1.68 | 65.18 |
| Horn | 1289 | 46 | 24.43 | 13.5 | 1.71 | 359.9 |
| Horn | 3535 | 37 | 145 | 78 | 1.7 | 1372 |

VI. DISCUSSION

Impedance matrix interpolation can be used to increase the computational efficiency of the method of moments. While simulation time improvements are made with small structures (less than 50 segments) the improvement in efficiency only becomes relevant with dealing with large structures over wide bandwidths. Broadband antennas such as the LPDA and horn antenna are well suited to the use of impedance matrix interpolation, however to obtain a wide enough bandwidth numerous sub-bands may be required resulting in discontinuities. This may be acceptable as MBPE is used in infancy of the design process where computational efficiency is traded for accuracy. In general it is possible to extrapolate to higher frequencies than is predicted by the method in Section III however not lower, this is especially true when input impedance is of concern. As input impedance is calculated on a single segment the effect of segments with large interaction distances have little effect on the solution. However when calculating radiation patterns the extrapolation range should not be exceeded as all the segment currents are used in the far field calculation. Simulation efficiency improvement of approximately 1.7 can generally be expected. When simulating electrically small structures the time again, in seconds, is not significant however when the problem size is large and many frequency points are of interest the use of impedance matrix interpolation results in a large reduction in simulation time.

A possible extension to the method is to treat each fitting function separately. The polynomial coefficients would be calculated from samples for the specific element before sampling the next element. This would reduce the additional storage

required, as impedance matrix sample need not be stored. Another benefit of this method is that the sample range for all the fitting function samples need not be the same. The sample range could then be specified per element, depending on interaction distance and connection, as to achieve the most accurate fitting function.

VII. CONCLUSION

Two impedance matrix interpolation methods have been effectively implemented in *SuperNEC* as a form of MBPE. The standard method approximates all the elements in the matrix with quadratic functions directly and an improved method where the dominant frequency variation terms is removed prior to approximation. The impedance matrix is then filled from the simpler fitting functions this reducing the simulation time as the fitting function is evaluated with less computational expense than direct computation. Choice of correct sample points is important in obtaining an accurate fitting model, the sample range can be determined by the maximum interaction distance of the structure, the centre frequency and simulation range. Curves were developed to obtain a relationship between simulation range and sample range. Given correct sample and simulation ranges a mean root square error of less than 10% can be expected of the entire range and significantly less error when the input impedance is the only parameter of interest. To extend the simulation bandwidth the band should be split up into sub bands, thus reducing the problem size for each of the sub-bands by segmenting at a highest frequency of the band. The use of impedance matrix interpolation methods have been found to be 1.7 times faster than using direct *SuperNEC* computation providing enough frequency points are of interest to make up for the time used in sampling the matrix and solving fitting function coefficients.

REFERENCES

- [1] R. F. Harrington. *Field Computations by Moment Methods*. New York: McMillan, 1968.
- [2] J. D. Kraus. *Antennas*. McGraw-Hill, 2nd ed., 1988.
- [3] E. K. Miller. "Model-Based Parameter Estimation in Electromagnetics: Part I. Background and Theoretical Development." *IEEE Antennas and Propagation Magazine*, vol. 40, no. 1, pp. 42–51, FEB 1998.
- [4] E. K. Miller. "Model-Based Parameter Estimation in Electromagnetics: Part II. Application to the EM observable." *IEEE Antennas and Propagation Magazine*, vol. 40, no. 2, pp. 51–65, APR 1998.
- [5] E. K. Miller. "Model-Based Parameter Estimation in Electromagnetics: Part III. Applications to EM Integral Equations." *IEEE Antennas and Propagation Magazine*, vol. 40, no. 3, pp. 49–65, JUN 1998.
- [6] G. J. Burke, E. K. Miller, S. Chakrabarti and K. Demarest. "Using Model-Based Parameter Estimation to Increase the Efficiency of Computing Electromagnetic Transfer Functions." *IEEE Transactions on Magnetics*, vol. 25, no. 4, pp. 2807–2809, JUL 1989.
- [7] J. Walsh. *Interpolation and Approximation by Rational Function in the Complex Domain*, chap. 3. American Mathematical Society, 5 ed., 1969.
- [8] D. H. Werner and R. J. Allard. "The simultaneous interpolation of antenna radiation patterns in both the spatial and frequency domains using Model-Based Parameter Estimation." *IEEE Transactions on Antennas and Propagation*, vol. 48, no. 3, pp. 383–392, MAR 2000.
- [9] N. I. O'Leary. *A SuperNEC Implementation of Model Based Parameter Estimation by Interpolating the Method of Moments Impedance Matrix*. MSc(Eng) Dissertation, University of the Witwatersrand, Johannesburg, 2006. Appendix D: Radiation pattern MBPE.
- [10] D. H. Werner and R. J. Allard. "The antenna Model-Based Parameter Estimation radiation patterns Using Windowed Interpolation and Spherical Harmonics." *IEEE Transactions on Antennas and Propagation*, vol. 51, no. 8, pp. 1891–1905, AUG 2003.
- [11] G. J. Burke and A. Poggio. *Numerical Electromagnetics code (NEC) - Method of Moments*. Lawrence Livermore Laboratory, January 1981.
- [12] D. R. Wilton and C. M. Butler. "Effective Methods for Solving Integral and Integro-Differential Equations." *Electromagnetics*, vol. 1, pp. 289–308, 1981.
- [13] E. Newman. "Generation of Wide-Band Data from the Method of Moments by interpolating the Impedance Matrix." *IEEE Transactions on Antennas and Propagation*, vol. 36, no. 12, pp. 1820–1824, DEC 1988.
- [14] K. L. Vigra and Y. Rahmat-Samii. "Efficient Wide-Band Evaluation of Mobile Communications Antennas Using [z] or [y] Matrix Interpolation with the Method of Moments." *IEEE Transactions on Antennas and Propagation*, vol. 47, no. 1, pp. 65–76, JAN 1999.
- [15] T. Sarkar, K. Siarkiewicz and R. Stratton. "Survey of numerical methods for solution of large systems of linear equations for electromagnetic field problems." *IEEE Transactions on Antennas and Propagation*, vol. 29, no. 6, pp. 847–856, NOV 1981.
- [16] J. Yeo and R. Mitta. "An Algorithm for Interpolating the Frequency Variations of Method-of-Moments Matrices Arising in the Analysis of Planar Microstrip Structures." *IEEE Transactions on Microwave Theory and Techniques*, vol. 51, no. 3, pp. 1018–1025, MAR 2003.
- [17] V. P. J. Yeo, S. Köksöy and R. Mitta. "Efficient Generation of Method of Moments Matrices Using the Characteristic Function Method." *IEEE Transactions on Antennas and Propagation*, vol. 52, no. 12, pp. 3405–3410, DEC 2004.
- [18] D. Nitch. *A serial and parallel design of NEC2 to demonstrate the advantages of the object-oriented paradigm in comparison with the procedural paradigm*. Ph.D. thesis, School of Electrical Engineering, University of the Witwatersrand, 1992.
- [19] A. Fourie and D. Nitch. "SuperNEC: Antenna and Indoor-Propagation Simulation Program." *IEEE Antennas and Propagation Magazine*, vol. 42, no. 3, pp. 31–48, JUN 2000.
- [20] M. R. A. Rubinstein, R. Rachidi and B. Revsler. "A Parallel Implementation of NEC." *IEEE Transactions on Electromagnetic Compatibility*, vol. 45, no. 2, pp. 177–188, MAY 2003.
- [21] N. I. O'Leary. *A SuperNEC Implementation of Model Based Parameter Estimation by Interpolating the Method of Moments Impedance Matrix*. MSc(Eng) Dissertation, University of the Witwatersrand, Johannesburg, 2006. Appendix A: Theory and Method.
- [22] C. J. Reddy, M. D. Deshpande, C. R. Cockrell, and F. B. Beck. "Fast RCS Computation over a Frequency Band Using Method of Moments in Conjunction with Asymptotic Waveform Evaluation Technique." *IEEE Transactions on Antennas and Propagation*, vol. 46, no. 8, pp. 1229–1232, AUG 1998.
- [23] E. Barbeay. *Polynomials*, chap. 7. Springer - Verlag, 1989.
- [24] Poynting Innovations. *SuperNEC MoM Technical Reference Manual*, 2.9 ed.
- [25] Poynting Innovations. *SuperNEC Input User Reference Manual*, 2.9 ed.
- [26] N. I. O'Leary. *A SuperNEC Implementation of Model Based Parameter Estimation by Interpolating the Method of Moments Impedance Matrix*. MSc(Eng) Dissertation, University of the Witwatersrand, Johannesburg, 2006. Appendix C: Error Analysis.
- [27] C. A. Balanis. *Antenna Theory: Analysis and Design*, chap. 11. John Wiley and Sons, 2 ed.
- [28] J. Kerr. "Short axial length broad-band horns." *IEEE Transactions on Antennas and Propagation*, vol. 21, no. 5, pp. 710–715, SEP 1973.
- [29] E. K. Miller and G. J. Burke. "An overview of some selected topics in computational electromagnetics: Present status and future directions." In *SAIEE Joint Symposium on Antennas and Propagation and Microwave Theory and Techniques*, pp. 1–10. August 1986.
- [30] N. I. O'Leary. *A SuperNEC Implementation of Model Based Parameter Estimation by Interpolating the Method of Moments Impedance Matrix*. MSc(Eng) Dissertation, University of the Witwatersrand, Johannesburg, 2006. Appendix B: Efficiency Analysis.
- [31] T.K Sarker, K. R. Siarkiewicz, and R.F Stratton. "Survey of numerical methods for solution of large systems of linear equations in electromagnetics." *IEEE Transactions on Antennas and Propagation*, vol. 38, no. 1, pp. 847–856, JAN 1981.

Part II

Appendices

Appendix A

Impedance Matrix Interpolation Theory and Method

A.1 Introduction

Calculation of wideband electromagnetic observable information is a computationally expensive task when using frequency domain methods such as the method of moments. This is because the simulation is to be performed at each frequency interval of interest. Much of computational time is in the filling of the impedance matrix, an $N \times N$ matrix also referred to as the mutual impedance matrix. As the observable parameters are difficult to predict themselves a method of interpolating the impedance matrix has been employed make the filling of the impedance matrix more efficient. As the elements in the impedance matrix vary predictably over frequency the elements are approximated with quadratic functions. This appendix contains the theory used in the method of moment and the method used to interpolate the impedance matrix. Three interpolation methods are proposed, a standard method where all the elements are approximated with quadratic function directly. An improved method, where the frequency variant componet has been removed before approximation. Thirdly a windowing method, where the impedance matrix elements are approximated with overlapping piecewise polynomial functions multiplied by a hann window function to remove discontinuities. Their implementation in *SuperNEC* is discussed as well as memory analysis performed.

A.2 Model-Based Parameter estimation

MBPE has been explained by Miller in [1] as a form of “cleaver” curve fitting, unlike standard methods of curve fitting the fitting model is chosen with physics of the problem in mind. When applied to problems in Computational Electromagnetics (CEM) MBPE is used to reduce computational time required to calculate required observable parameters such as antenna input impedance, VSWR and radiation (electric far field) pattern [2]. In EM design, the value of these parameters are required over a wide frequency band. Frequency domain EM solver methods such as the Methods of Moments (MoM) and Finite Element Modelling (FEM) require the problem to be solved at each frequency point of interest, making them computationally expensive methods to obtain wide-band information.

Since EM observable parameters generally vary unpredictably with frequency it is difficult to estimate the values using standard methods of interpolation and extrapolation, like polynomial approximation and Taylor series. Thus methods have been employed to approximated these variables and still produce accurate results. Rational functions can be employed to accurately represent EM parameters over frequency, these function have the ability to model “nulls”, generally encountered when dealing with EM problems over a wide frequency band. Another methods is to approximate a predicable function used in the calculation with a simple approximation techniques. If less computational effort is used in evaluating the fitted function than original function improvements can be made in simulation time without losing solution accuracy.

A.3 Method of Moments

The method of moments (MoM) is a numerical method to solve the electric field integral equation (EIFE) on perfect electrical conductors (PEC), for a detailed explanation of the method of moments see [3, 4, 5]. The EFIE, in (A.1), represents the electrical field due to a volume current distribution \vec{J} [6].

$$\vec{E}(\vec{r}) = \frac{-j\eta}{4\pi k} \int_v \vec{J}(\vec{r}') \cdot \vec{G}(\vec{r}, \vec{r}') dV' \quad (\text{A.1})$$

where:

$$\begin{aligned}
\overline{\overline{G}}(\vec{r}, \vec{r}') &= (k^2 \overline{\overline{I}} + \nabla \nabla) g(\vec{r}, \vec{r}') \\
g(\vec{r}, \vec{r}') &= \frac{e^{(-jk|\vec{r}-\vec{r}'|)}}{|\vec{r}-\vec{r}'|} \\
k &= \omega \sqrt{\mu_0 \varepsilon_0} \\
\eta &= \sqrt{\frac{\mu_0}{\varepsilon_0}}
\end{aligned}$$

In order to reduce above vector integral to a scalar integral the thin wire approximation is used. The assumption is made that the current flow axially only on the wire, a filament current scalar I replaces the surface current vector \vec{J} . The field integral in (A.1) is now reduced to the one in (A.2), also know as Pollockington's equation.

$$\hat{s} \cdot \vec{E}^I = \frac{j\eta}{4\pi k} \int_L I(s') \left(k^2 \hat{s} \cdot \hat{s}' - \frac{\delta^2}{\delta s \delta s'} \right) g(\vec{r}, \vec{r}') ds' \quad (\text{A.2})$$

where:

$$\begin{aligned}
s &= \text{distance parameter along wire axis at } r \\
s' &= \text{distance parameter along wire axis at } r'
\end{aligned}$$

The primary field ($\hat{s} \cdot \vec{E}^I$) can be the excitation on the structure or an incident plane wave on the structure [7]. The current $I(s')$ is solved by splitting the structure into N pieces or segments as expressed in (A.3)

$$I(s') = \sum_{n=1}^N \alpha_n f_n(s) \quad (\text{A.3})$$

Where α_n are the unknown constants and $f_n(s)$ a set of weighting or basis functions. By substituting into (A.2) we obtain the N^{th} order linear system:

$$\sum_i Z_{mn} \alpha_n = E_m \quad m = 1, 2 \dots N \quad (\text{A.4})$$

$[Z]$ is the $N \times N$ impedance matrix, where the row and column are represented by subscripts m and n respectively. The element Z_{mn} represents the mutual impedance between the observation segment m and testing segment n [8].

$$Z_{mn} = \frac{j\eta}{4\pi k} \int_L f_n(s) K(r_m, r') ds' \quad (\text{A.5})$$

$$K(r_m, r') = \frac{\delta^2}{\delta s \delta s'} g(r_m, r') + k^2 g(r_m, r') \quad (\text{A.6})$$

where the free space Green's function:

$$g(r_m, r') = \frac{e^{-jk|\vec{r}_m - \vec{r}'|}}{|\vec{r}_m - \vec{r}'|} \quad (\text{A.7})$$

Various choices exist for the testing functions $f_n(s)$, The testing funitons used in the Numerical Electromagnetic Code (NEC) are the Sine, Cosine and Constant basis functions shown in (A.8).

$$f_n(s) = A_i + B_i \text{sink}(s - s') + C_i \text{cosk}(s - s') \quad (\text{A.8})$$

A detailed explanation of the implementation of these testing functions can be found in [6, 9].

A.3.1 SuperNEC

SuperNEC is an implementation of the Numerical Electromagnetic Code (NEC) originally developed by Lawrence Livermore Laboratories [6]. The code and theory was reimplemented in C++ by Derek Nitch [9] in 1987. The object-oriented nature of the code made it easy to modify and extend. Extensions have included an Uniform Geometric Theory of Diffraction (UTD) Method of Moments hybrid [10] and fast iterative solver methods. Other additions include a parallel implementation such that simulation can be run on multiple computers on a local area network (LAN) [11].

One of *SuperNEC*'s advantages is the Matlab input-output graphical user interface(GUI). With the aid of the Matlab environment a user can run batch simulation, varying input parameters in order to optimise output observables. Wire grid models, such as metal structures and antennas, can easily be generated with the aid of SIG (structure interpolation and gridding) [12]. A genetic algorithm (GA) antenna optimising tool was developed by Brandon Orchard [13], which interfaces with *SuperNEC* via Matlab.

The formulation of MoM shown in *Section A.3.1* imposes restrictions on the structure used in the simulation and the way it is segmented. In order to obtain an accurate solution when using the method of moments it is important to ensure that the structure is segmented correctly. Segmentation in *SuperNEC* is performed by the input GUI however it is important to ensure that the model frequency is set to the highest frequency point of interest [14]. The conditions for producing a well segmented structure are shown in *Tables A.1* and *A.2*, where Δ , λ and a are segment length, simulation wavelength and radius respectively.

Table A.1: Guidelines for length and radius of individual segments [14]

| Segment condition | Error |
|--------------------------------|------------------------------|
| Length to wavelength condition | $\Delta > \frac{\lambda}{5}$ |
| Radius to wavelength condition | $\frac{\lambda}{a} < 30$ |
| Length to Radius ratio | $\frac{\Delta}{a} < 0.5$ |

Table A.2: Guidelines for length and radius at segment junctions [14]

| Segment condition | Error |
|------------------------|---|
| Length ratio | $\frac{\Delta_{\max}}{\Delta_{\min}} > 5$ |
| Radius ratio | $\frac{a_{\max}}{a_{\min}} > 10$ |
| Length to Radius ratio | $\frac{\Delta}{a} < 2$ |

A.4 Impedance matrix interpolation

Impedance matrix interpolation as a MBPE method was implemented on dipole thin wire antenna structures by Newman [15] and later by Vigna and Rahmat-Samii [16] on more complex communications antennas. Both of these implementation used a quadratic function to approximate the elements in the impedance matrix ($[Z]$) over the frequency range of interest. The underlying principle in impedance matrix MBPE is that the elements in the impedance matrix vary predictably over a specified frequency range. Consider the 1m wire dipole antenna in *Figure A.1*, which has been segmented into 27 pieces each 0.04m in length with a constant 0.01m radius. The antenna input impedance is shown in *Figure A.2*, we can clearly see that the input impedance varies too much to be approximated by a polynomial or Taylor series. A rational function fitting model could be used however the order and sample points would need to be chosen correctly, as is the case with radiation pattern interpolation [17]. If we now consider the impedance matrix elements $Z_{1,2}$, $Z_{1,12}$ and $Z_{1,22}$ shown in *Figure A.3*. Element $Z_{1,2}$ represents the mutual impedance between the first and second segments, 0.037 metres apart, $Z_{1,12}$ is the mutual impedance between the first and

twelfth elements, 0.44 metres apart and $Z_{1,22}$ is mutual impedance between the first and twenty second segment, 0.81 metres apart. As the interaction distance increases as does the variation over frequency of the impedance matrix elements. However the element's variation is predictable over frequency and can easily be approximated by a polynomial function.

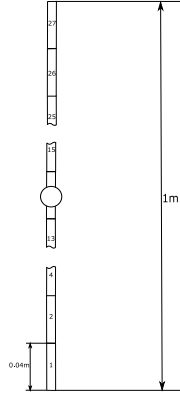


Figure A.1: Dipole antenna with 27 Segments

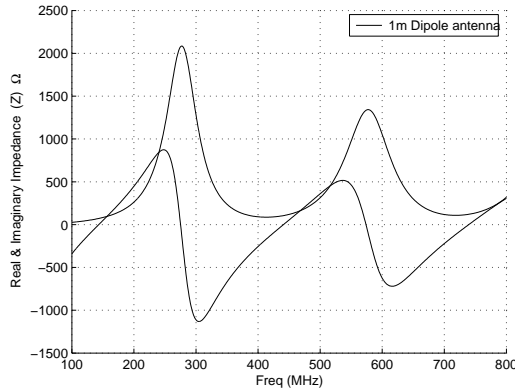


Figure A.2: Input impedance of 1 metre dipole antenna

(A.5) is used to calculate the impedance matrix elements, the sine, cosine and constant testing functions $f_n(s)$ vary little over frequency. The Green's function in (A.7) is largely effected by the interaction distance of the source and observations points. By keeping this distance small the elements in the impedance matrix can easily be approximated by a quadratic function.

As the the impedance matrix is an $N \times N$ matrix filled with complex values, $2N^2$ fitting functions would be required. Two K^{th} order polynomial functions are used to approximate each of the impedance matrix elements. The real and imaginary components are treated separately hence two function are required as shown in (A.9). To determine the polynomial coefficients the at least $K+1$ samples of the impedance matrix must be taken. Samples of the impedance matrix are obtained by filling the matrix using the standard MoM method, these samples are stored and used in the computation of the impedance matrix fitting functions.

$$Z_{m,n}(f) = (a_K f^K + \dots + a_1 f + a_0) + (b_K f^K + \dots + b_1 f + b_0)i \quad (\text{A.9})$$

The method of least squares [18] was initially used to solve for the polynomial coefficients. This method was chosen as it is flexable as to the order of the polynomial as well as the number of sample points taken. Using a higher order polynomial function one could produce a better fit on the impedance matrix elements and hence a more accurate final solutions.

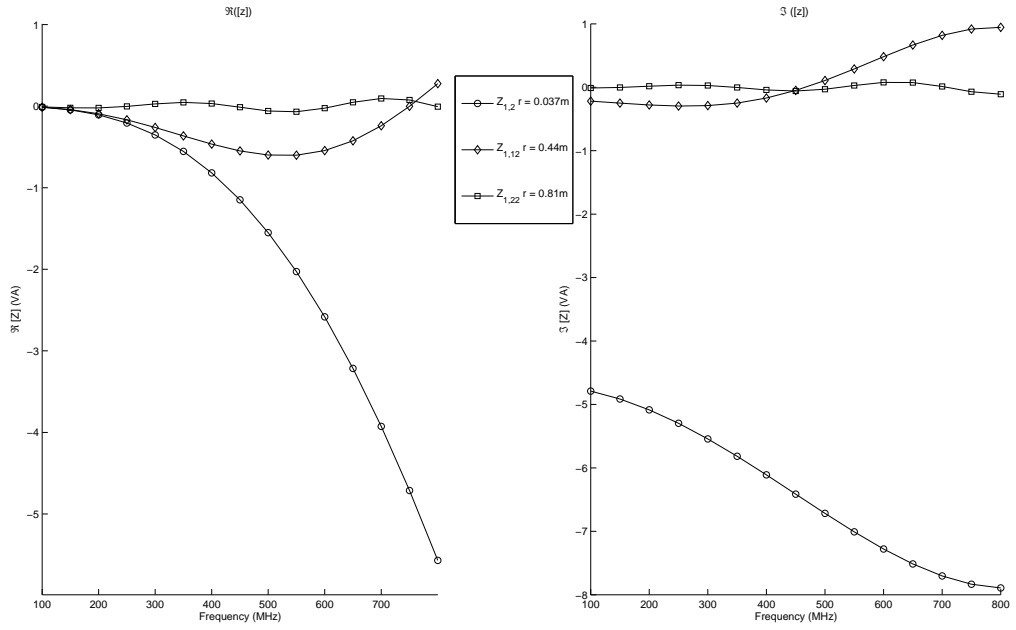


Figure A.3: Real and Imaginary components of three impedance matrix elements over frequency

The ability to sample more than the minimum number of points gives the ability to vary the sample range without losing accuracy in the fit. A detailed explanation of the least squares method can be found in *Section A.4.1*.

Preliminary testing on arbitrary structures showed that when approximating the impedance matrix elements with a polynomial the dominant factor in obtaining an accurate approximation was the sample range. *Figure A.4* shows the current mean square relative error over the $200 - 700\text{MHz}$ frequency range for a 0.5m dipole antenna with increasing sample range. The error converges at the minimum for any number of samples points used. For this reason the method of least squares replaced by a faster but less flexible method of calculating the coefficients for a 2^{nd} order polynomial by sampling the impedance matrix at three points and solving the resulting linear system.

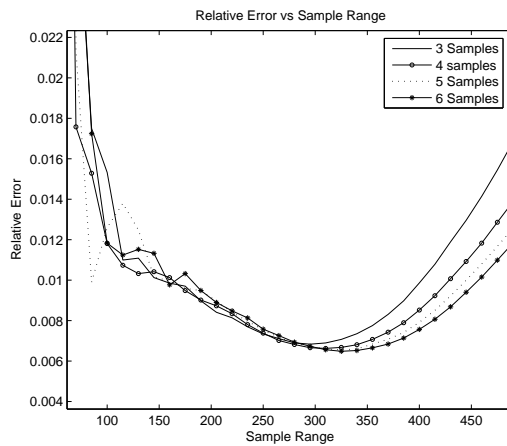


Figure A.4: Error in impedance matrix when approximated by a 2^{nd} order polynomial vs sample range, for various number of samples used

A.4.1 Method of Least Squares

The method of least squares is a method of fitting a k^{th} order polynomial to a data set K samples large. This is done by reducing the sum of the mean square error. For a more details explanation of the least squares method can be found in [19]. The polynomial coefficients are determined by solving the linear system below:

$$\begin{bmatrix} K & \Sigma x & \Sigma x^2 & \dots & \Sigma x^k \\ \Sigma x & \Sigma^2 x & \Sigma x^3 & \dots & \Sigma x^{k+1} \\ \Sigma x^2 & \Sigma^3 x & \Sigma x^4 & \dots & \Sigma x^{k+1} \\ \vdots & \vdots & \vdots & \vdots & \vdots \\ \Sigma x^k & \Sigma^{k+1} x & \Sigma x^{k+2} & \dots & \Sigma x^{2k} \end{bmatrix} \begin{bmatrix} a_0 \\ a_1 \\ a_2 \\ \vdots \\ a_k \end{bmatrix} = \begin{bmatrix} \Sigma y \\ \Sigma xy \\ \Sigma x^2 y \\ \vdots \\ \Sigma x^k y \end{bmatrix} \quad (\text{A.10})$$

A.4.2 Windowing

The above method is only accurate over a narrow frequency band as the polynomial approximation of the impedance matrix loses accuracy with extrapolation past the centre frequency. A method proposed to counteract this effect is to use multiple polynomial function to approximate the impedance matrix elements over a wide frequency band. Each of the polynomial function is calculated from points sampled within a smaller frequency band. Filling of the impedance matrix is then performed by evaluating the polynomial function specified for the current frequency range.

$$f(x) = \begin{cases} f_1(x) & \text{for } 0 \leq x_1 \\ f_2(x) & \text{for } x_1 < x \leq x_2 \\ \vdots & \\ f_n(x) & \text{for } x_{n-1} < x \leq x_n \end{cases} \quad (\text{A.11})$$

Discontinuities will result if the functions are implemented one after another as in (A.11). To counteract this overlapping polynomials multiplied by a window function used. Each of the functions are overlapped in a way such that the sum of the window functions will equal one. A N point Hann window function is used as the overlapping window function, evaluated by :

$$w(n) = 0,5 \left(1 - \cos \frac{2\pi n}{N-1} \right) \quad (\text{A.12})$$

Second order polynomial functions are used for each of the window intervals. To reduce the number of samples required and any discontinuities between the functions sample point sharing is used. This is achieved by using the last sample point used in calculating the first polynomial as the first sample point for the second polynomial, and so on. The window will then extend from the first sample point used for the given function to the last. A slightly different approach is used for the first and last windows, the first window function will equal one to the point where the second function begins. From this point the first window will become the second half of the Hann window as in (A.12). This procedure is illustrated *Figure A.5*, where three window functions are overlapped. It is shown that the sum of the window functions results in one over the entire range.

Applying this method to the impedance matrix elements produce an accurate fitting model. *Figure A.6(a)* shows the $\Re \{Z_{1,1}\}$ element of the impedance matrix approximated by three piecewise quadratic functions, multiplied by the above window function. The approximation is better than when using a single quadratic function, however not dramatically as the impedance matrix elements does not vary largely over the frequency range. *Figure A.6(b)* shows the $\Re \{Z_{1,20}\}$ element approximated using the same procedure outlined above, greater frequency variation is attributed due to the greater interaction distance between the source and observation segment. Using three windowed functions now shows a large improvement in the accuracy obtained by the approximating function when compared to using a single quadratic function.

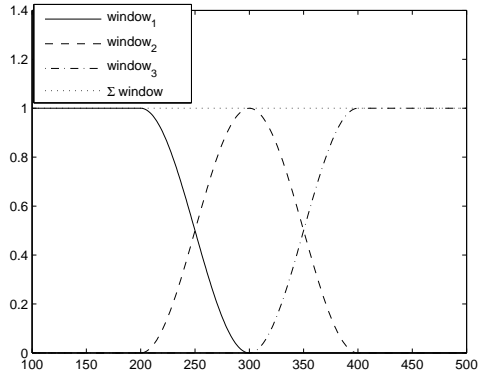


Figure A.5: Three overlapping Hann window functions

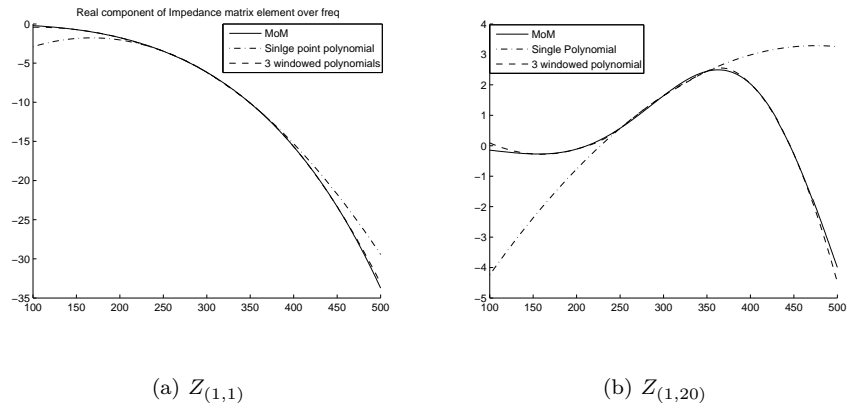


Figure A.6: Impedance matrix elements approximated by piecewise windowed quadratic functions and a single quadratic function

A.4.3 Improved interpolation

The general method used to improve impedance matrix interpolation schemes is to remove the dominant frequency variation term. [15, 16, 20, 21] show that the elements in the impedance matrix are proportional to $e^{-j2\pi\lambda\vec{R}}$ where \vec{R} is the centre to centre distance between the source and observation segments. By removing this term from each of the impedance matrix elements, as in (A.13), the frequency variation of the impedance matrix terms are reduced significantly.

$$[Z]' = \frac{[Z]}{e^{-j2\pi\lambda\vec{R}}} \quad (\text{A.13})$$

The MBPE scheme is now to interpolate the new $[Z]'$ matrix once the variant term has been removed. This term is re-introduced when the impedance matrix is evaluated from the polynomial functions by evaluating the inverse of (A.13).

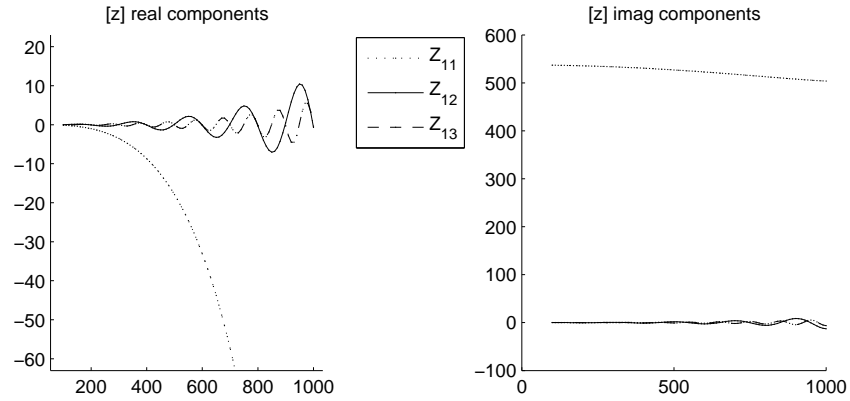


Figure A.7: Real and Imaginary component of three impedance matrix elements over a wide frequency band

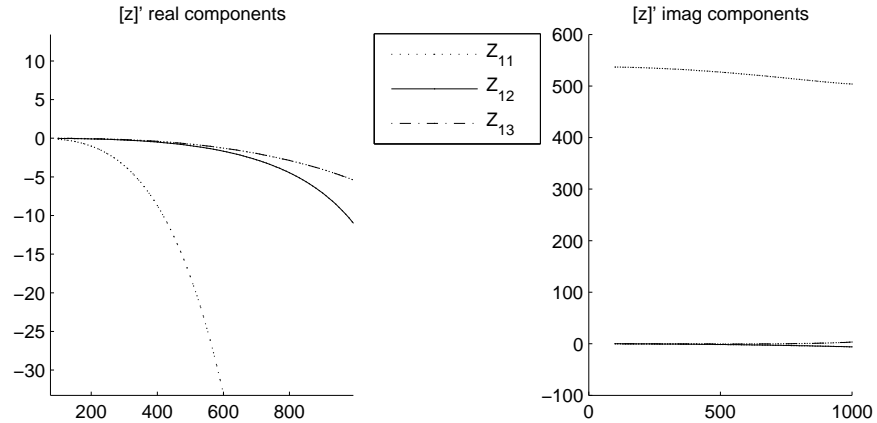


Figure A.8: Real and Imaginary component of three $[Z]'$ matrix elements over a wide frequency band

Figure A.7 shows three impedance matrix elements over a wide frequency band, one can clearly see the oscillatory component introduced by the $e^{-j2\pi\lambda\vec{R}}$ term in both the Real and Imaginary components. This component has been removed in Figure A.8, the elements of $[Z]'$ vary predictably over frequency and can easily be approximated by a low order polynomial such as a quadratic function.

A.4.4 *SuperNEC* implementation

All three of the above impedance matrix interpolation schemes were implemented in the *SuperNEC* C++ code. Due to the object-oriented nature of the *SuperNEC* code additional functionality can be added while still having the standard method available for testing and code benchmarking. As the *SuperNEC* source code is large the OO nature of the code made it possible to easily access the parts of the code which were needed for the implementation of the MBPE methods. These parts were the input file reading code and the matrix filling methods. *SuperNEC* has various matrix filling procedures including the direct method and spares methods, the impedance matrix code was only applied to the direct matrix filling case. However there is scope to apply MBPE to the other filling methods.

The polynomial and improved interpolation methods will be explained first as they use the same input file format and the evaluation process is similar.

Standard and Improved impedance matrix interpolation

The input .NEC file is used to input the parameters of the MBPE simulation, these parameters are:

- Number of sample points
- Order of polynomial approximation
- Frequency at which samples are taken
- Method used to determine coefficients

These parameters are included in the NEC file as follows:

```
FS  NOSAMPLES
FR  0    1    0    0    0    0    0    0    0    0    0    0    0    0    0    0    0    0    0    0    0
EX  0    1    1    0    0    1.00000  0.00000
XQ
FR  0    1    0    0    0    0    0    0    0    0    0    0    0    0    0    0    0    0    0    0
EX  0    1    1    0    0    1.00000  0.00000
XQ
FR  0    1    0    0    0    0    0    0    0    0    0    0    0    0    0    0    0    0    0    0
EX  0    1    1    0    0    1.00000  0.00000
XQ
IT  ORDER  METHOD
```

Where the FS card indicates that the impedance matrix interpolation method is to be used and the argument NOSAMPLES specifies the number of samples to be used. FR is the standard NEC frequency card and is used to specify the sample frequency. EX and XQ are the standard excitation and execute cards respectively. Note that the number of FR, EX and XQ cards used must equal NOSAMPLES specified for the simulation. IT tells the code to calculate the polynomial coefficients, ORDER specifies the order of the polynomial to be used. METHOD specifies the method used to calculate the polynomial coefficients being either 0 Least squares method or 1 the analytical method. If the analytical method is used only a second order polynomial can be used and only three impedance matrix samples are required. Checks have been implemented to ensure that parameters specified will result in a valid simulation.

This code is included after the geometry cards and before the simulation parameters are specified, for more information on the NEC input file structure see [6, 14]. Presently these are included in the NEC file manually, code could be included in the Matlab frontend to specify and write these parameters.

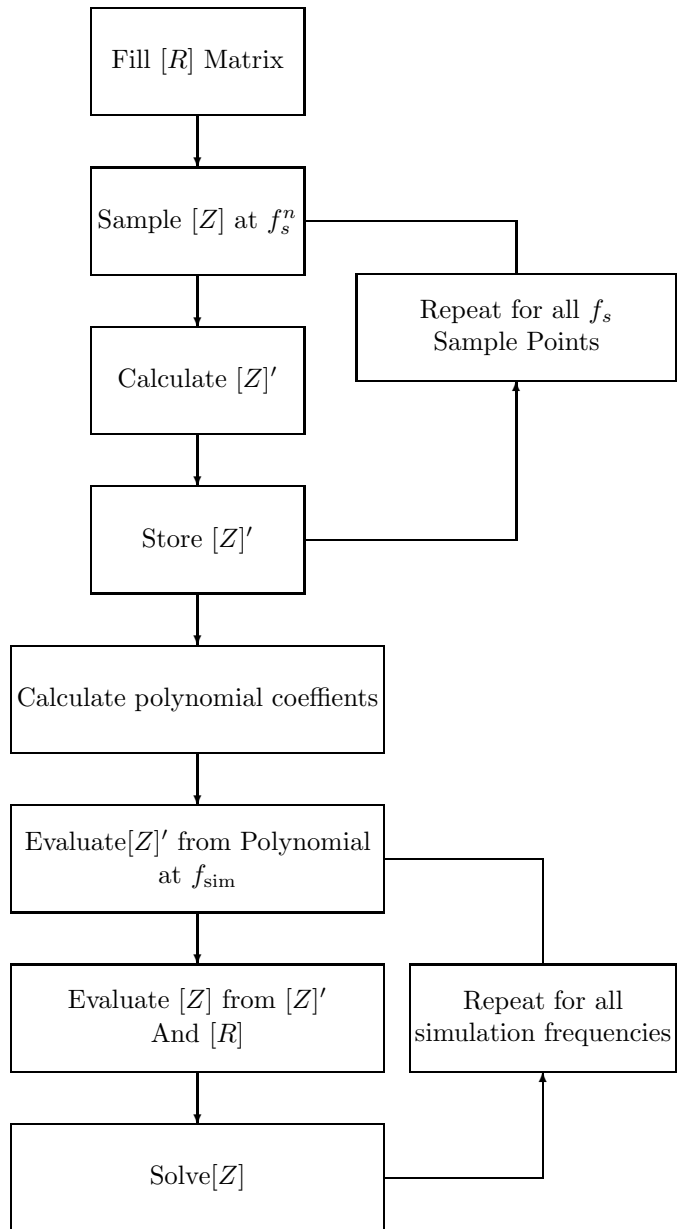


Figure A.9: Flow diagram of improved interpolation scheme

The flowchart in *Figure A.9* shows the process in the improved interpolation method. The $[R]$ matrix represents a matrix of interaction distances between testing and observation segments. The impedance matrix is sampled at the specified sample frequency points, each of these samples is converted to the $[Z]'$ matrix via the calculation in (A.13). Once all the samples have been obtained the polynomial coefficients are calculated using the method specified in the input NEC file and stored in a $N \times N \times (k + 1)$ complex matrix, this matrix is referred to as the coefficient matrix. Filling of the impedance matrix is then achieved by evaluating each of the polynomials at each frequency point of interest and the variant component re-introduced by evaluating the inverse of (A.13). Once the impedance matrix has been filled it is solved using the standard *SuperNEC* method.

The method used in standard interpolation is the same with the exception of filling the $[R]$ matrix, removing and re-introducing the resonant component. The polynomial fitting functions are obtained using the impedance matrix samples.

Windowed polynomial interpolation

The windowed polynomial method uses a similar method to input the simulation parameters as the above methods. All parameter information is specified in the input NEC file, the format of the windowing commands is as follows:

```
WI   STARTFREQ   ENDFREQ   NOWINDOWS
```

As before this information is inserted after the geometry information and before the simulation information. WI specifies that the windowing method is to be used, STARTFREQ and ENDFREQ specify the first and last frequency points respectively. NOWINDOWS is the number of window functions to be used over the specified frequency range. The sample points are then calculated by the code such that point-sharing can be done. A second order polynomial is used for each interval using three impedance matrix samples to calculate the coefficients, the number of impedance matrix samples is calculated by:

$$N_s = (2N_{\text{windows}} + 1) \quad (\text{A.14})$$

To obtain the sampling frequency rate (Δf) :

$$\Delta f = \left[\frac{2 \times \text{TotRange}}{N_{\text{windows}} + 1} \right] \quad (\text{A.15})$$

where:

$$\begin{aligned} \text{TotRange} &= \text{ENDFREQ} - \text{STARTFREQ} \\ N_{\text{windows}} &= \text{NOWINDOWS} \end{aligned}$$

Recalculation of the impedance matrix elements is done by evaluating all the quadratic functions multiplied by the window function. Due to the complex nature of the windowing method no simulation time improvement is obtained in the use of the method and hence no efficiency or accuracy analysis had been done.

A.4.5 Storage

As impedance matrix samples along with polynomial coefficients need to be stored it is worth discussing the memory required in their storage. The impedance matrix consists of complex values with a large numerical range as can be seen in *Figure A.3*, two floating point (*float*) variables are used to express the Real and Imaginary components of the value. Four bytes of memory are required to store a single *float* value, hence eight bytes is used for each impedance matrix element. $8N^2$ bytes is used in storing entire impedance matrix, while $8N^2 \times N_s$ is used in storing N_s samples of the matrix.

A single matrix element fitting model is represented by $k+1$ complex values, thus $8N^2(k+1)$ bytes are used to store the coefficient matrix. The memory used to store the impedance

matrix can only be freed once the coefficients have been calculated hence the maximum amount of additional memory used ,in bytes, for the standard impedance matrix interpolation technique is:

$$\text{MEM}_{\max} = 8N^2 (N_s + k + 1) \quad (\text{A.16})$$

The only additional memory requirement when using the improved method is the inclusion of the $[R]$ matrix. A single *float* value is used to for each of the elements in the matrix. Thus (A.16) can be modified to include this component:

$$\text{MEM}_{\max}^{\text{improved}} = 8N^2 (N_s + k + 1.5) \quad (\text{A.17})$$

The windowing method requires significantly more memory than the other two methods as a polynomial matrix must be stored for each of the domains. The memory used in specifying the window function is small compared to the memory used in storage, thus is not considered in this analysis. One method used to reduce the amount memory needed is to only store the impedance matrix samples required in the calculation of the specific polynomial function. The maximum additional memory required, in bytes, is:

$$\text{MEM}_{\max}^{\text{window}} = 8N^2 (3 \times N_{\text{win}} + 4) \quad (\text{A.18})$$

Figure A.10 shows the amount of additional memory used in the impedance matrix interpolation schemes, three samples with a second order polynomial fitting model have been used for the standard and improved method while three window functions are used in the windowing method. As the problem size increases the amount of memory increase dramatically, for this reason it has been not possible to use the windowing method on problems sizes exceeding a few hundred unknowns.

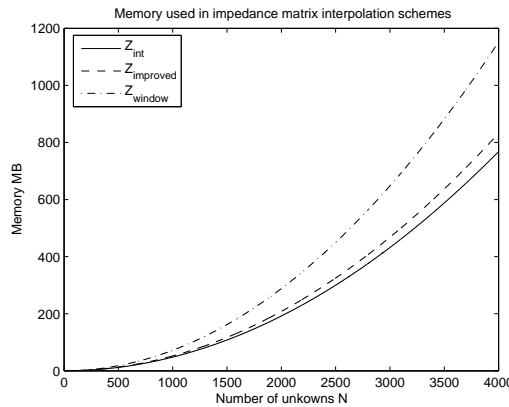


Figure A.10: Additional memory used in the impedance matrix MBPE methods

A.5 Conclusion

The filling of the impedance matrix in the method of moments is a computationally expensive task. This process can be made more efficient by interpolating the impedance matrix by approximating the the elements in the matrix with simple function. The standard interpolation method uses quadratic functions to approximate the impedance matrix elements, three samples must be obtained to determine the coefficients of the fitting functions. This method is adequate over narrow frequency bands with electrically small structures. The improved method removed the frequency variant component $e^{-j2\pi\lambda\vec{R}}$, where \vec{R} is the interaction distance between segments, before the fitting functions are calculated. This improved method allows the impedance matrix interpolation to be applied to large structures over greater frequency bands. A method of using multiple polynomial functions over sub-bands was also implemented. Each of the overlapping sub-bands where approximated by a quadratic

function multiplied by a Hann window function to remove discontinuities between band. The implementation of these MBPE methods in *SuperNEC* increases the amount of memory required in the simulation, it was found that the standard and improved methods use approximately $40N^2$ bytes of additional memory and the windowing method uses an additional $8N^2(3 \times N_{win} + 4)$ bytes, where N_{win} is the number of sub-bands. Efficiency analyses of the standard and improved method can be found in [22] and accuracy analysis in [23].

References

- [1] E. K. Miller. “Model-Based Parameter Estimation in Electromagnetics: Part I. Background and Theoretical Development.” *IEEE Antennas and Propagation Magazine*, vol. 40, no. 1, pp. 42–51, FEB 1998.
- [2] J. D. Kraus. *Antennas*. McGraw-Hill, 2nd ed., 1988.
- [3] R. F. Harrington. *Field Computations by Moment Methods*. New York: McMillan, 1968.
- [4] R. F. Harrington. “Matrix Methods for Field Problems.” *Proceedings of the IEEE*, 1967.
- [5] A. Djordjevic and T. Sarkar. “A Theorem on the Moment Methods.” *IEEE Transactions on Antennas and Propagation*, MAR 1987.
- [6] G. J. Burke and A. Poggio. *Numerical Electromagnetics code (NEC) - Method of Moments*. Lawrence Livermore Laboratory, January 1981.
- [7] S. Gee, E.K. Miller, A.J. Poggio, E.S. Selden and G.J. Burke . “Computer Techniques fo Electromagnetic Scattering and Radiation Analyses.” *IEEE Electromagnetic Compatibility Symposium Record*, JUL 1971.
- [8] J. H. Richmond. “Radiation and Scattering by Thin-Wire Structures in the Complex Frequency Domain.” Tech. rep., OSU Research Foundation, 1973.
- [9] D. Nitch. *A serial and parallel design of NEC2 to demonstrate the advantages of the object-oriented paradigm in comparison with the procedural paradigm*. Ph.D. thesis, School of Electrical Engineering, University of the Witwatersrand, 1992.
- [10] A. Fourie and D. Nitch. “SuperNEC: Antenna and Indoor-Propagation Simulation Program.” *IEEE Antennas and Propagation Magazine*, vol. 42, no. 3, pp. 31–48, JUN 2000.
- [11] Poynting Innovations. *SuperNEC Parallel MoM User Reference Manual*, 2.7 ed.
- [12] Poynting Innovations. *SuperNEC SIG GUI Manual*, 1.0 ed.
- [13] B. Orchard. *Optimising Alorithms for Antenna Design*. MSc(Eng) Dissertation, University of the Witwatersrand, Johannesburg, 2002.
- [14] Poynting Innovations. *SuperNEC Input User Reference Manual*, 2.9 ed.
- [15] E. Newman. “Generation of Wide-Band Data from the Method of Moments by interpolating the Impedance Matrix.” *IEEE Transactions on Antennas and Propagation*, vol. 36, no. 12, pp. 1820–1824, DEC 1988.
- [16] K. L. Vigra and Y. Rahmat-Samii. “Efficient Wide-Band Evaluation of Mobile Communications Antennas Using [z] or [y] Matrix Interpolation with the Method of Moments.” *IEEE Transactions on Antennas and Propagation*, vol. 47, no. 1, pp. 65–76, JAN 1999.

- [17] N. I. O’Leary. *A SuperNEC Implementation of Model Based Parameter Estimation by Interpolating the Method of Moments Impedance Matrix*. MSc(Eng) Dissertation, University of the Witwatersrand, Johannesburg, 2006. Appendix D: Radiation pattern MBPE.
- [18] R. L. Lafara, editor. *Computer Methods for Science and Engineering*. Intertext Books, 1973.
- [19] P. J. Davis. *Interpolation and Approximation*, chap. 2. Blaisdell Publishing Company, 1 ed., 1963.
- [20] J. Yeo and R. Mittra. “An Algorithm for Interpolating the Frequency Variations of Method-of-Moments Matrices Arising in the Analysis of Planar Microstrip Structures.” *IEEE Transactions on Microwave Theory and Techniques*, vol. 51, no. 3, pp. 1018–1025, MAR 2003.
- [21] V. P. J. Yeo, S. Köksoy and R. Mittra. “Efficient Generation of Method of Moments Matrices Using the Characteristic Function Method.” *IEEE Transactions on Antennas and Propagation*, vol. 52, no. 12, pp. 3405–3410, DEC 2004.
- [22] N. I. O’Leary. *A SuperNEC Implementation of Model Based Parameter Estimation by Interpolating the Method of Moments Impedance Matrix*. MSc(Eng) Dissertation, University of the Witwatersrand, Johannesburg, 2006. Appendix B: Efficiency Analysis.
- [23] N. I. O’Leary. *A SuperNEC Implementation of Model Based Parameter Estimation by Interpolating the Method of Moments Impedance Matrix*. MSc(Eng) Dissertation, University of the Witwatersrand, Johannesburg, 2006. Appendix C: Error Analysis.

Appendix B

Impedance Matrix Interpolation Error Analysis

B.1 Introduction

Ultimately the accuracy of MBPE will determine how useful it is as a method to increase the computational efficiency of the Method of Moments (MoM). If the method cannot accurately approximate the observable parameters required for design, it would not be of great use in the design process. In any approximation method, a certain amount of accuracy is lost, however, knowing how accurate the method is also of great importance. It is important to quantify the accuracy loss in the method such that the designer can make informed decisions when using the optimisation tool. In impedance matrix interpolation, there are many variables which will determine the error in the observable; these include interaction distance, sample range, simulation range, number of unknowns in the structure, and segmentation of the structure. This appendix aims to give a guide to a designer as to what the best sample range and simulation ranges should be used for specific maximum interaction distances. Various specific antenna cases have been simulated using the determined sample range, and the results analysed. The concept of a confidence interval is introduced, a frequency band around the centre frequency where the model can be used confidently. Only the standard and improved interpolation methods are analysed in this section; the windowing method is shown to not produce an increase in simulation efficiency and hence is not regarded as a usable MBPE method. For the figures and tables in the following sections, $MBPE_1$ refers to the standard interpolation method and $MBPE_2$ the improved interpolation method; for the details of the theory and implementation of these methods, see [1].

B.2 Error Analysis Method

Model fitting can be done for specific cases, however, this is often not useful as a general case. Impedance matrix interpolation schemes can be implemented on any MoM structure, however, the error will not be the same for all cases. Since it is impossible to test every possible structure case, a few structure properties relate to obtainable accuracy when using MBPE; these properties include source observation distance, number of unknowns in the structure (segments), and how these segments are connected within the structure.

Impedance matrix interpolation schemes approximate each of the elements in the impedance matrix with a simpler function over frequency. The most obvious method of specifying the error would be to give it in terms of the error between the fitting model and the actual value. This would be meaningless as the impedance matrix is not only large, it also does not relate to any observable parameter used in EM design. Furthermore, the impedance matrix is inverted and multiplied by the excitation vector to obtain a solution for the structure currents. Thus, specifying the error of the impedance matrix elements would be misleading, as a small deviation in impedance matrix values may result in a large solution error. An observable parameter must then be used to quantify the error in the solution; input impedance could be used, however, the input impedance generally only relates to a single segment. If one were to consider an antenna mounted on an airplane, the currents on the end of the wing would have little effect on the input impedance of the antenna but may have a larger effect on the radiation pattern of the antenna. Structure currents have been chosen as the observable parameter to quantify the error; it is the direct solution of the MoM procedure. Once again, it is difficult to look at the error for all the currents in the structure individually, hence an average of all the currents is used. Thus, the root square error as a function of frequency is defined by:

$$e(f) = \frac{1}{N} \sqrt{\sum_{k=1}^N \frac{|I_k - I_k^m|^2}{|I_k|^2}} \quad (\text{B.1})$$

This gives the root square relative error of all the currents in the structure at a specific frequency. Relative error has been used instead of absolute error as a norm value, as it gives a more intuitive error value. The effect of phase offset in the solution when using absolute error is disproportionately increased, while the root mean error gives a realistic error.

Using this information it is possible to determine the accuracy over any frequency range of interest. An average error over a specific frequency band is defined by:

$$\|e\| = \frac{1}{n_f} \sum_{f=1}^{n_f} e(f) \quad (\text{B.2})$$

B.3 Sampling

Choosing the correct sampling frequencies is critical in obtaining an accurate solution, it is important to note that there will never be a standard sampling frequency. One will always have to take into account the structural properties and the frequency range over which the observable is required. Acceptable error is also an important consideration, it is possible to trade accuracy for a wider observation range in frequency, in which case a wider sampling range should be used. This would generally be the tradeoff as MBPE methods are used as a “first step” in EM design as wide band information can be generated faster than using the direct method. However the designer may wish to decrease the acceptable error and run the simulation over a narrower band to refine the design in specific bandwidths. When using these MBPE methods one would have the advantage of being able to generate observable parameters at more frequency intervals such that finer information of the frequency band in question can be obtained.

The method used for determining the sampling rate in [2, 3] is to restrict the maximum phase shift in the $e^{-j2\pi\lambda\vec{r}_{mn}}$ term [1] to π . Hence for a maximum centre to centre separation in the structure R_{\max} the interpolation step size is found to be:

$$\Delta f_s = \frac{f_{\max}}{2 \left(\frac{R_{\max}}{\lambda} \right)} \quad (\text{B.3})$$

Where f_{\max} is the maximum frequency point of interest. Note this equation gives the sample frequency in terms of λ and hence the must be multiplied by the centre wavelength. This method of determining the sample frequency can be used well as a guide however does not necessarily ensure that the optimum sample range. The variant term $e^{-j2\pi\lambda\vec{r}_{mn}}$ has been removed from the sampling data in the improved interpolation scheme and hence this method, while not producing inaccurate results, may not be the best method for determining the sample range for the improved method. One advantage of using (B.3) is that it relates the sample range to the upper frequency limit, however as the results in [3] showed that the frequency range can easily be too wide to produce sufficiently accurate results. The method used was to reduce the range into two sub-domains, a similar technique to the windowing method [1]. Sample range as a function of interaction distance was tested to find on optimum sample range. A three segment structure was tested, with the segments being vertically aligned and with increasing separation. The maximum separation in the structure is the centre to centre distance of the two further most segments. The segment length to wavelength ratio was performed at the maximum solution frequency [4] as to avoid any additional errors caused by an invalid structure. As a starting point the simulation was performed in single MHz steps ranging from 200to400 MHz with a centre frequency of 300 MHz . The code was then tested using both methods with a varying sample range, the sample range which produced the lowest mean error over the range was noted. (B.2) is used to determine the mean error over the frequency range specified. Figure B.1 shows the sample range which achieved the minimum solution mean relative error, the results for both method differ from those predicted by the theoretical values. However the variation in the point where minimum solution error occurs, especially for the improved interpolation case, shows that this result cannot provide a sufficiently predictable relationship to determine best sample range.

[3] specified that a sampling range of less than (B.3) should be used to produce accurate results, however never specified how much less for each case. In order to produce a dynamic solution to any problem a reliable method must be obtained to to determine the sampling

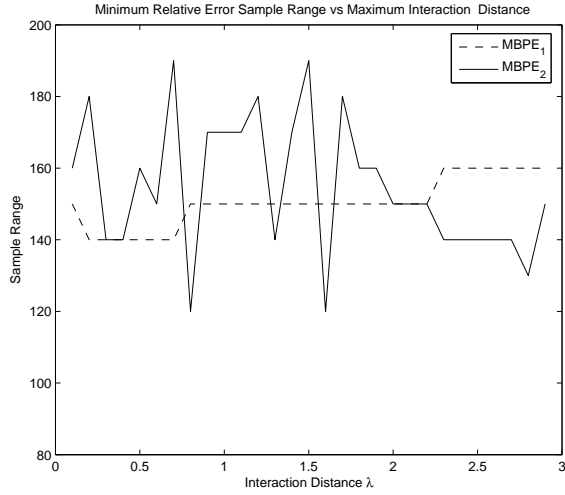


Figure B.1: Sample range where minimum mean relative error occurs with increasing interaction distance

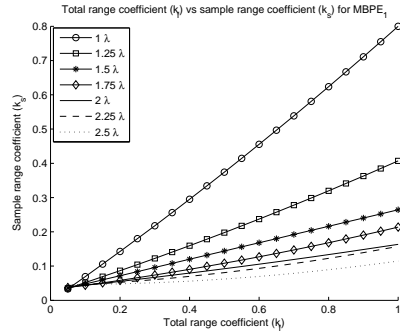
range. A slight variant of the (B.3) is used and shown in (B.4), the difference being is that the sample range is now relative to the centre frequency and a factor k_s is introduced. This factor will be different for various cases. The simulation frequency is then specified by (B.3) where k_f is a constant to relate the simulation frequency range to the equation.

$$\Delta f_s = k_s \times \frac{f_{\text{centre}}}{2 \left(\frac{R_{\text{max}}}{\lambda} \right)} \quad (\text{B.4})$$

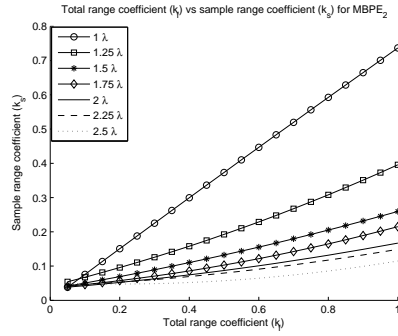
$$f_M = k_f \times \frac{f_{\text{centre}}}{\left(\frac{R_{\text{max}}}{\lambda} \right)} \quad (\text{B.5})$$

The each of the two constants (k_s and k_f) in the above equations were varied and the MBPE method tested with the calculated frequency range and sample range using (B.5) and (B.4) respectively. Direct computation was used over the same frequency such that the error in the MBPE simulation could be calculated. This was done for various cases of maximum interactions distance. The sample range which produced the minimum error for each of the simulation ranges was noted, this procedure was continued for increasing interaction distance. The resulting curves produce a form of look-up table which can be used to determine the sample frequency which should be used for a given simulation range and interactions distance, as to produce the most accurate solution. The above coefficients are thus obtained by the curves in Figure B.3. For cases with a maximum interaction distance of less than 1λ the sample range became too large, these cases should be treated as if the maximum interaction distance is 1λ . The results show that sample range coefficient (f_s) converges to 0.05 past a maximum interaction distance of 3λ . Note that the simulation range is still specifies by the user, however is related to the simulation range coefficient by means of (B.5). If the value of k_f is greater than 1 the simulation range should be split into smaller sub-ranges., this method is discussed later.

The average root mean error over the performed simulation range is shown in Figure B.3, these curves are for maximum interaction distance. Note that the error obtained in these curves must only be used as a guide, the exact error value is depend on more parameters than the interaction distance itself. However these curves show for which simulation ranges acceptable error can be obtained. Figure B.3(a) show that the standard interpolation method should not be used with a simulation range coefficient greater than 0.4 while the improved method produces acceptable error over the entire range.

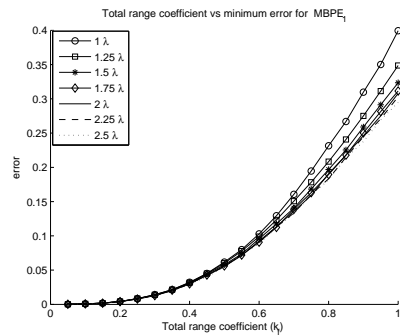


(a) MBPE₁

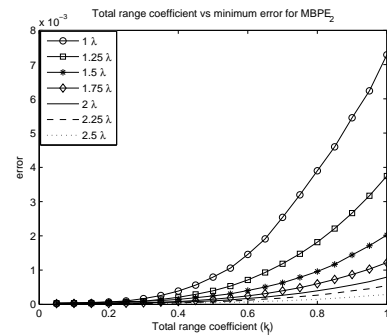


(b) MBPE₂

Figure B.2: Simulation range coefficient (f_s) versus Sampling coefficient (k_s) for optimum sample range



(a) MBPE₁

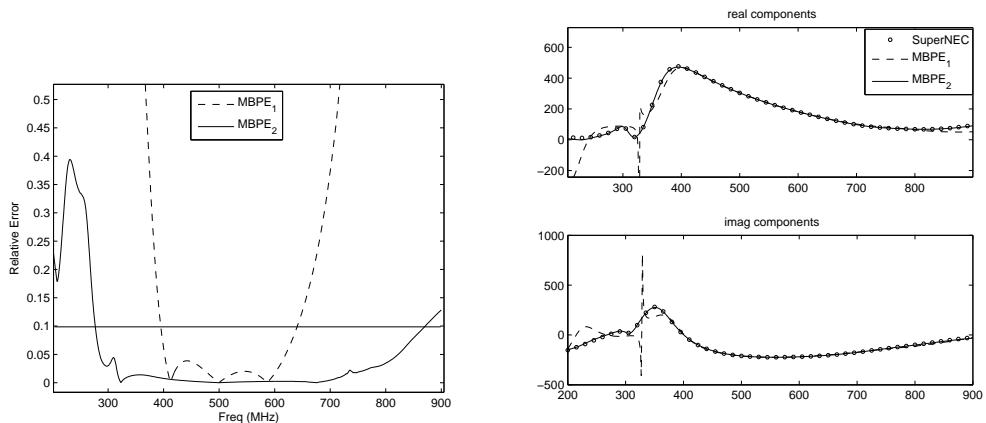


(b) MBPE₂

Figure B.3: Simulation range coefficient (f_s) versus average Root mean error over the simulation range

B.4 Confidence interval

The confidence interval is defined as the the frequency range over which the impedance matrix can be interpolated while reproducing sufficiently accurate results in the solution. In order to define this range must specify an acceptable error (or cut-off limit) in the solution. When dealing with the extrapolation range the error tends to be fairly constant over a certain range then increase drastically at two points, these are the upper and lower limits of the interpolation range. Consider the mean relative current error shown in *Figure B.4(a)* both interpolation methods show a drastic increase in error when extrapolating past a certain point if frequency. The horizontal line represents 10% error in the solution, this has been chosen as the cut-off limit to determine the extrapolation range. However as the *Figure B.4(a)* shows, if the cut-off limit is decreased it would not have a large effect the confidence interval. This is especially true of the standard interpolation scheme and the lower limit of the improved method. The upper limit of the improved method generally extends further than the lower one, however as a guide the same cut-off limit is used to determine the confidence interval.

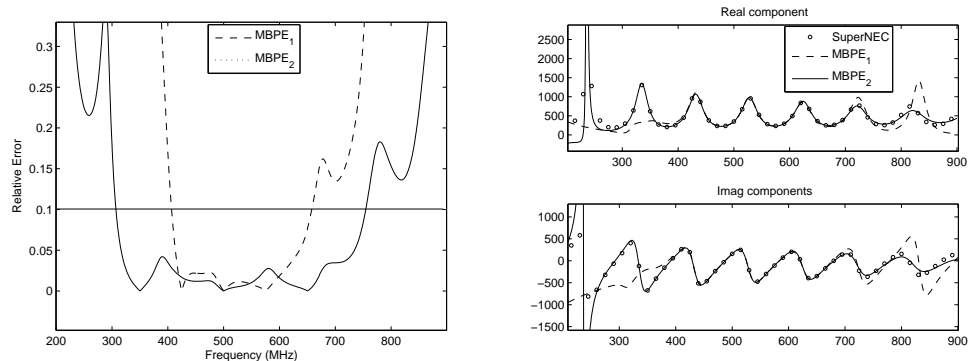


(a) Mean relative current error over frequency,
 $R_{\max} = 1.7\lambda f_c = 500MHz$

(b) Input impedance, MBPE methods compared
to direct *SuperNEC* computation

Figure B.4: Mean relative current error and input impedance over frequency for Yagi antenna

As mentioned before the MoM solution error is not only a function of interaction distance, number of unknowns and frequency range. The characteristics of the antenna effect the solution, as the error is being calculated on the observable parameter current, the variation in the waveform must be considered when specifying how well any fitting model performs. *Figure B.4(a)* shows the relative error of the currents in a Yagi structure, *Figure B.4(b)* shows input impedance of this antenna of the simulated range it is clear that the impedance varies relatively slowly over frequency. By contrast consider the input impedance of a highly resonant structure such as a loop antenna [5] in *Figure B.5(b)*, the input impedance varies significantly more over frequency. Both structure have a similar number of segments and maximum interaction distance. Comparing the mean relative current error in Figures B.4(a) and B.5(a) the loop antenna case shows a slightly narrower confidence interval than was the case with the Yagi antenna. It is important to note that although the performance on the MBPE method is slightly worse for a structure with more variation in the observable it is still significantly better than using a general fitting model on the observable itself [6].



(a) Mean relative current error over frequency, $R_{\max} = 1.6\lambda$, $f_c = 500MHz$ (b) Input impedance, MBPE methods compared to direct *SuperNEC* computation

Figure B.5: Mean relative current error and input impedance over frequency for Loop antenna

B.5 Effect of specific simulation and structure properties

B.5.1 Error as a function of separation distance

As the elements in the impedance matrix become more variant it is important to quantify how accurate the use of the MBPE methods are with increasing interaction distance. For this three separate segments were used space equally apart, with the source segment in the centre. The gaps between the segments were increased for each simulation and the error between the MBPE and standard *SuperNEC* solutions noted. The sample range was chosen at $200MHz$ and the simulation was run in single MHz increments over the same range. The choice of sample range was arbitrarily selected to determine how the method performs with a standard set of parameters.

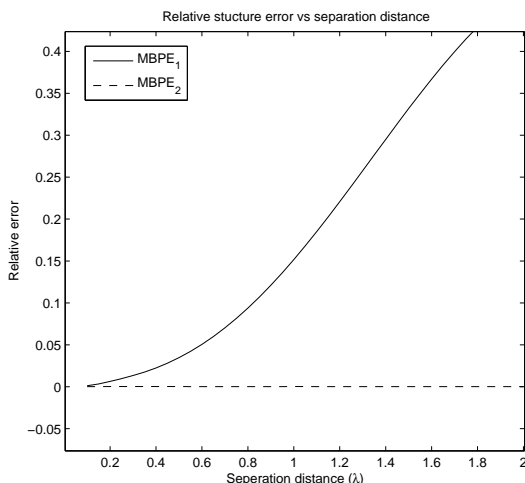


Figure B.6: Relative error vs interaction distance of three segments structure

Figure B.6 shows the mean relative error over the frequency range versus the interaction distance of the two furthest segments in the structure. One can clearly see that the performance the improved interpolation scheme is significantly better than the standard

method. Almost no increase in error is obtained when the interaction distance is increase opposed to a quadratic increase in error with the standard case.

B.5.2 Affect of problem size on solution accuracy

As the interaction distance has a profound effect on the accuracy of the standard interpolation method only the improved method will be considered as it is difficult to increase the problem size without increasing maximum interaction distance. It was shown in *Section B.5.1* that the as the maximum interaction distance had little effect on the solution accuracy given the method in *Section B.3* was used to determine the sample range.

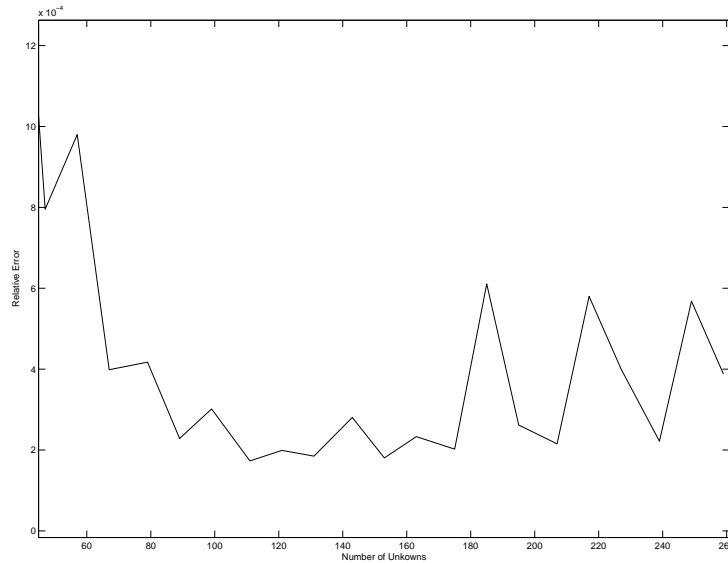


Figure B.7: Graph showing average relative error for increasing number of structure unknowns

Figure B.7 shows that there is no trend in relating MoM problem size to the accuracy of the impedance matrix interpolation method. This curve was generated by increasing the length of a wire structure such that the number of unknowns increased. Since the length of the structure increased so did the maximum interaction distance, as method in *Section B.3* was used to determine both the sample range and simulation range these parameters were not constant for all the length cases. The constants k_f and k_s were set to 0.8 and 0.4 respectively. The example shown here validates that the method for determining the sample and simulation ranges is correct as the error tends to be constant over the increasing interaction distance.

B.5.3 Error due to incorrect structure segmentation

Due to the assumptions used in the NEC formulation [7] various segmentation restrictions are placed on the structure to take the assumptions into account. These restrictions limit the length and radius of segments for the given wavelength for both individual segments and segments junctions, the restrictions are outlined in [1, 4]. While simulating an illconditioned structure using direct *SuperNEC* computation will produce an inaccurate solution, the use of impedance matrix interpolation on the same structure will compound the error. The solid line in *Figure B.8* represents direct *SuperNEC* computation with the structure segmented at the maximum frequency. The dotted line is the *SuperNEC* solution with an undersegmented structure. The input impedance obtained when using improved interpolation on

the undersegmented structure is shown by the dashed line. The interpolation method here performs worse than it would if the correct segmentation had been used.

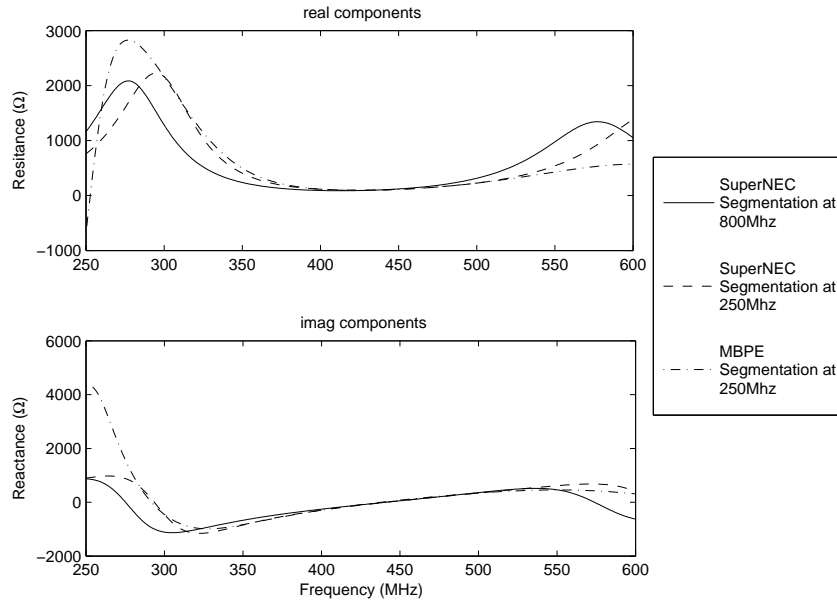


Figure B.8: Input impedance of dipole antenna produced by *SuperNEC* with correct segmentation, incorrect segmentation and improved interpolation with incorrect segmentation

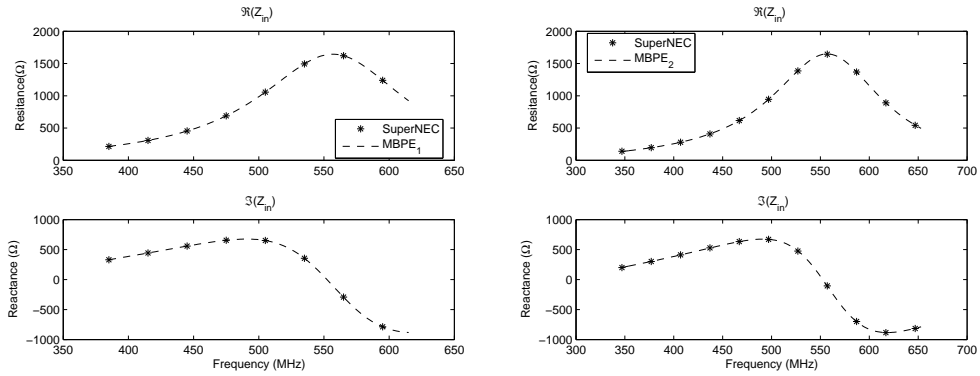
In order to produce the best possible solution it is important that the structure is segmented at the maximum frequency of interest and not the centre frequency. To ensure this is achieved the *SuperNEC* structure checker should be used before performing any simulations [4]. The higher the segmentation frequency to more unknowns are introduced into the problem. As MBPE is a method to reduce the simulation time simulation may be more efficient to simulate over multiple frequency band with separate segmentation frequencies than simulate over the entire band with the maximum segmentation. In order to determine whether this method would be more efficient one must consider the simulation time as a function of number of unknowns and frequency points of interest as shown in [8].

B.6 Specific antenna cases

To truly quantify the performance these optimisation methods they must be applied to test case structures. Each antennas in the following sections where chosen as they introduce specific elements to the simulation both in structure and observable. The antennas chosen are electrically large wire structures as they perform well with in *SuperNEC* , microstrip antennas and electrically small antennas have been omitted as *SuperNEC* does not handle these types of structures particularly well. The current version of *SuperNEC* does not have the ability to include dielectrics to the structure, a case which impedance matrix interpolation has been applied to with good results [3, 9]

B.6.1 Dipole Antenna

As the dipole antenna is the one of the most simple antenna type in terms structure and observable parameters it is a good choice to use in benchmarking. The dipole antenna used was $0.5m$ dipole antenna with a centre frequency of $500MHz$. Segmentation was done at a frequency of $800MHz$ as to ensure that errors due to incorrect segmentation where not introduced.



(a) MBPE₁

(b) MBPE₂

Figure B.9: Input impedance of 0.5m dipole antenna via direct *SuperNEC* computation and MBPE methods

Figure B.9 shows the input impedance of the dipole antenna calculated with the use of the standard *SuperNEC* direct computation method and the MBPE methods. Both methods show good agreement with those produced by direct computation. The variation in this case is low as is maximum interaction distance being only 0.83λ . Consider average the error in all the segments in Figure B.10, the error value is below 10% for the all of the simulation range in the standard interpolation case and only above the value at the extremities for the improved case. A wider simulation range was used for the improved method however the same range could have been used for the standard method due to the small interaction distance of the segments, with the maximum distance being less than 1λ .

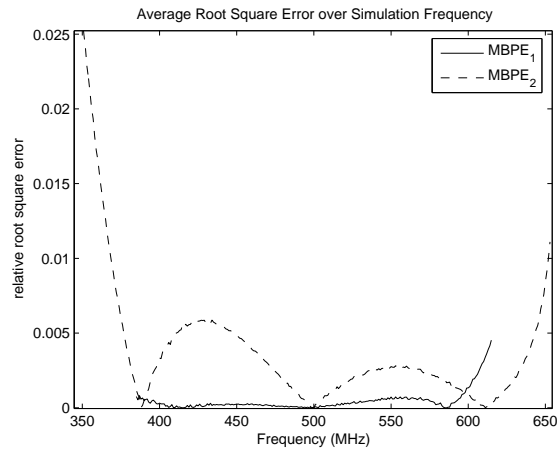


Figure B.10: Root square structure current error over simulation range for dipole antenna

Table B.1 contains the simulation sample range and simulation range coefficients and the error obtained for the simulation. The improved method performed worse than the standard method, this is largely due to the fact that a larger sample range was used for the improved method and the interaction distance was kept low. For case such as this it would be advantages to use the standard method as it shows a greater improvement in simulation time. This is significant as less frequencies points where used in the standard case and if the same where used in both case the standard method would outperform the improved method further. However the increase in simulation time, in seconds, is so small that the using direct *SuperNEC* computation should be used.

Table B.1: Simulation parameters and results for dipole antenna

| | MBPE ₁ | MBPE ₁ |
|---------------------------------------|-------------------|-------------------|
| k_s | 0.45 | 0.58 |
| k_f | 0.6 | 0.8 |
| Number of Frequency points | 255 | 339 |
| Total average error (%) | 0.046437 | 0.40669 |
| Maximum error (%) | 0.45287 | 2.9366 |
| Confidence interval (MHz) | 201 | 307 |
| Mean error in confidence interval (%) | 0.046446 | 0.40669 |
| Total increase in simulation time (%) | 36 | 34 |

B.6.2 Yagi antenna

The complexity, both in structure and observable, is increased in simulating a Yagi antenna. A five element yagi antenna was used with the same centre frequency, of $500MHz$ as the case before. The maximum interaction distance of the simulated antenna was 1.3λ with 50 segments in the structure.

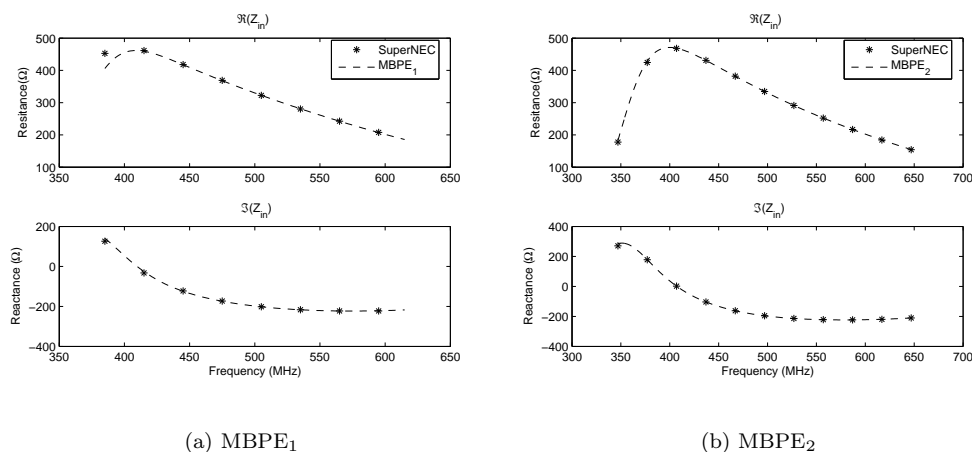


Figure B.11: Input impedance of five element yagi antenna via direct *SuperNEC* computation and MBPE methods

Figure B.11 shows the input impedance of the yagi antenna for both the MBPE cases with points generated by *SuperNEC* overlaid. The standard method now loses accuracy toward the lower end of the frequency band however reproduces the observable well on the upper range. The improved interpolation method accurately approximates the input impedance of the antenna over the entire simulation range being a wider range than the standard method.

The root mean structure current error is shown in Figure B.12, it is clear that the improved method outperforms the standard method with the entire simulation band being well below the 10% error level. The standard method produces a large error to the left of the centre frequency however is acceptable to the right. This is generally the case when simulating antenna cases with large interaction distances with the standard method. Table B.2 shows the parameters and results from the simulation. The improved method shows mean accuracy of 4.4% error over the entire range and 4.3% within the confidence interval. The confidence interval is more than double that of the standard case. For this reason if the input impedance is the observable of interest it may better to use the standard MBPE method over multiple smaller bandwidths as to have a greater reduction in simulation time. However if the entire solution is of importance as would be the case when looking at the radiation pattern the use of the improved method would be better, as the calculation of radiation pattern is done by taking all the segment currents into account [7].

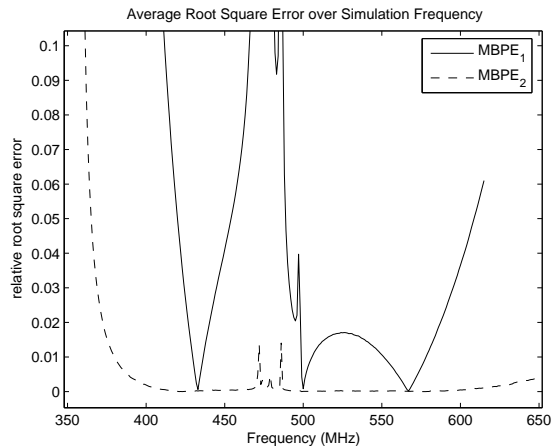


Figure B.12: Root square structure current error over simulation range for yagi antenna

Table B.2: Simulation parameters and results for yagi antenna

| | MBPE ₁ | MBPE ₁ |
|---------------------------------------|-------------------|-------------------|
| k_s | 0.35 | 0.4 |
| k_f | 0.6 | 0.8 |
| Number of Frequency points | 231 | 286 |
| Total average error (%) | 9.0876 | 4.448 |
| Maximum error (%) | 241 | 315.32 |
| Confidence interval (MHz) | 128 | 292 |
| Mean error in confidence interval (%) | 5.5 | 4.3 |
| Total increase in simulation time (%) | 51 | 53 |

B.6.3 Log periodic dipole array

The log periodic dipole array (LPDA) antenna is widely used in broadband applications. The structure is similar to that of the yagi antenna in the case above however transmission line connect the wire elements, this make for interesting results when using MBPE as currents are not only a function of interaction distance.

The input impedance of the antenna when using the standard interpolation method in *Figure B.13(a)* shows a poor approximation to the impedance generated by *SuperNEC*. The approximation is worse once again toward the lower end of the frequency range than the upper end. By contrast the improved method in *Figure B.13(b)* shows an well conditioned approximation to the input impedance generated by *SuperNEC*. The use of the improved interpolation scheme here would be the only reliable method, the root square current error in *Figure B.14* shows that the average error over all the structure the currents for the standard interpolation case is very erratic. While the improved case is not as good as was the case with other antenna cases it still shows a low level of error over the frequency range.

The radiation pattern of this poorly designed LPDA antenna shows a non-omnidirectional radiation pattern. The elevations radiation pattern of the antenna at $380MHz$ and $600MHz$ is shown in *Figures B.15(a)* and *B.15(b)* respectively. The standard interpolation method fails to approximate the pattern generated by direct computation while the improved method reproduces the curve such that the difference is not apparent. If the standard method was used in the design the results show a performance better than as it the real case, by contrast if the improved method is used the designer would get accurate results of how the antenna performs. The result of the simulation in *Table B.3* reiterate that only the improved method should be used for this antenna type, due not only to the greater interaction distance of the structure but the network connecting the elements. However the total sample range of the LPDA antenna should be decrease to produce better results than where achieved in this

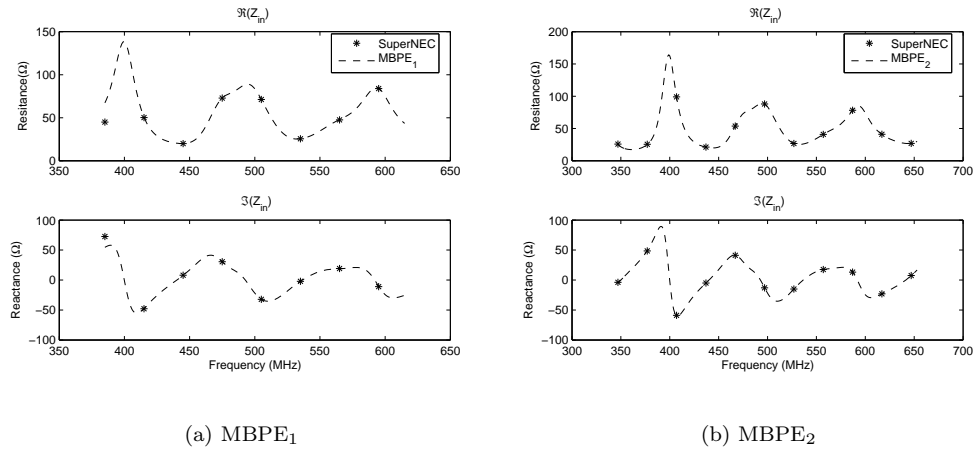


Figure B.13: Input impedance of LPDA antenna via direct *SuperNEC* computation and MBPE methods

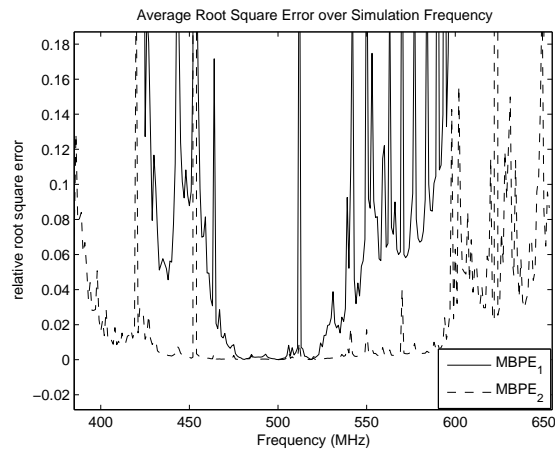


Figure B.14: Root square structure current error over simulation range for LPDA antenna

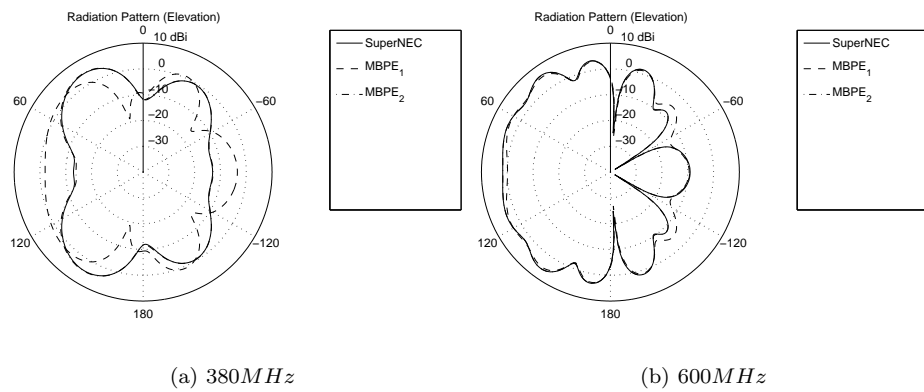


Figure B.15: Elevation radiation pattern of LPDA at 380 MHz and 600 MHz

case.

Table B.3: Simulation parameters and results for LPDA antenna

| | MBPE ₁ | MBPE ₁ |
|---------------------------------------|-------------------|-------------------|
| k_s | 0.1 | 0.1 |
| k_f | 0.6 | 0.8 |
| Number of Frequency points | 99 | 133 |
| Total average error (%) | 62 | 12 |
| Confidence interval (MHz) | 47 | 147 |
| Mean error in confidence interval (%) | 2.8 | 80 |
| Total increase in simulation time (%) | 41 | 39 |

With this structure the problem size, 221 unknowns, is large enough to produce a significant decrease in simulation time. Which makes this method a useful tool in determining EM observables. The increase in computational speed is worth the loss in accuracy when generating wide band information. Since the LPDA antenna is a wide band antenna [10] the improved interpolation method is a good choice for the first step in the design process.

B.6.4 Horn Antenna

The plate structures in the horn and horn waveguide introduce many segments into the structure. The horn antenna used in the simulation has 1289 segments, making the antenna another good candidate for impedance matrix interpolation as even generating narrow band information is a computationally expensive task. A large amount of simulation time can be reduced by the use of MBPE methods.

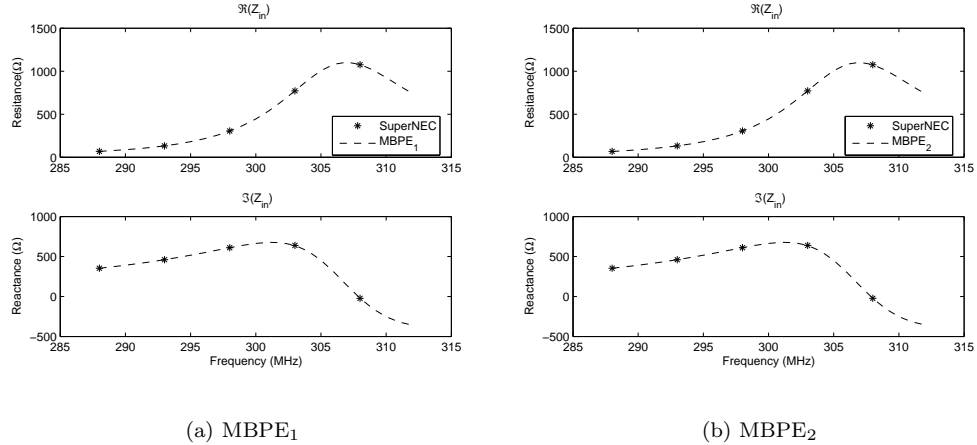


Figure B.16: Input impedance of horn antenna via direct *SuperNEC* computation and MBPE methods

Figure B.16 shows the input impedance of the antenna over the frequency band, a narrow frequency band was used due to the time required to simulate and structure of this size over a wide band. The input impedance generated by the MBPE methods again shows very little error over the simulation range.

The error over frequency shown in Figure B.17 shows a error of around 5% for most of the simulation range. The simulating range used was very narrow resulting in a very narrow sampling frequency range. It is expected that if the range was increased the improved method would perform well while the standard method would become very inaccurate.

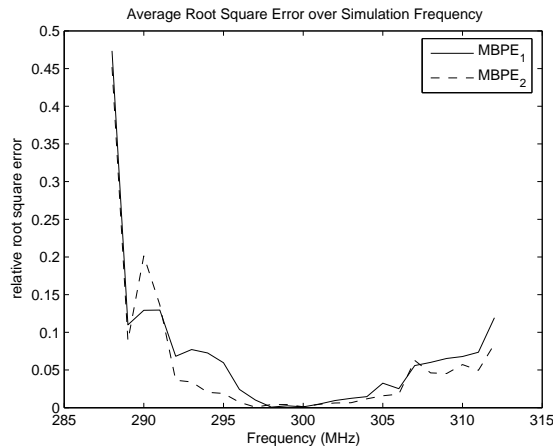


Figure B.17: Root square structure current error over simulation range for horn antenna

Table B.4: Simulation parameters and results for horn antenna

| | MBPE ₁ | MBPE ₂ |
|---------------------------------------|-------------------|-------------------|
| k_s | 0.05 | 0.05 |
| k_f | 0.3 | 0.3 |
| Number of Frequency points | 25 | 25 |
| Total average error (%) | 6.7 | 5.6 |
| Confidence interval (MHz) | 20 | 21 |
| Mean error in confidence interval (%) | 7.8 | 6.6 |
| Total increase in simulation time (%) | 40 | 36 |

B.6.5 UTD plate

The yagi antenna from the example in *Section B.6.2* was simulated with the addition of a UTD plate. The addition of the UTD plate greatly increases the simulation time. The formulation of the UTD used in *SuperNEC* can be found in [11], *SuperNEC* uses a UTD-MOM hybrid code such that UTD plates and cylinders can be included in a MoM structure. Simulation using UTD plates and cylinders is a time consuming task due to the brute force method used in calculating the path of the rays. While impedance matrix interpolation has not been developed directly to apply to the UTD case it can be used to interpolate in the impedance matrix with a UTD structure present. The $1m^2$ UTD plate is aligned vertically 0.2m behind the the yagi antenna, with the flat plane facing the backend of the antenna.

The input impedance calculated using the impedance matrix method in *Figure B.18* shows accuracy is lost toward the lower end of the frequency range. The error over frequency in *Figure B.19* also shows that the error is greater than other antenna case in prior examples. A high level of error is found around the centre frequency which can be attributes to the distance of the plate to the structure, which is around 0.5λ at the centre frequency. For this reason impedance matrix interpolation methods should not be applied to the UTD case directly. However if we consider the simulation time improvement of over 22 seconds for both the MBPE case it would should be a method to consider in the future. The UTD case is also generally used in the calculation of radiation patterns, impedance matrix interpolation methods do not increase the efficiency of the radiation pattern calculation other than in finding the structure currents. While impedance matrix interpolation methods could be applied to speed up this portion of the far field calculation it is a relatively fast process when compared to computing the far field itself. Impedance matrix interpolation method could be used in conjunction with UTD optimisation methods such as ray tracing, a method which had recently been applied in *SuperNEC* [12].

B.7 Analysis of results

From the results discussed it is shown that developing a general rule for determining the accuracy of the impedance matrix interpolation methods is not feasible. However it is possible to get *rule-of-thumb* method for determining where the solution was accurate for specific simulated structures and simulation ranges. The standard interpolation method should not be used for structures with maximum interaction distance of greater than a wavelength unless it is over a very narrow frequency band. Since the standard method shows a greater increase in simulation efficiency it may be an option to use the standard method over number smaller simulation ranges and adjust the structure segmentation accordingly. Discontinuities will result between the simulation band so this method must be used at the designers discretion. The improved method can be used for electrically large structures over wider bands with accurate results. From the cases above it is generally possible to extrapolate to higher frequencies than specified, but not lower frequencies. Simulation over a too wide range requires segmentation of the structures to a point where it may be more efficient to use the technique over smaller band, however discontinuities will result in the solutions. If the sub band approach is used with direct *SuperNEC* computation discontinuities would be expected as simulating with a differently segmented structure will yield different results. The discontinuities however would not be a great as with the MBPE methods as the dissimilar solution will be magnified by the inaccuracy in the approximation.

Antenna structure properties should also be considered when using impedance matrix interpolation methods. From the above antenna cases the LPDA antenna showed areas in frequency where the error was significantly greater than others. These areas of increased error can be attributed to the transmission lines in the structures. Remember that the impedance matrix is considered to be a matrix of mutual impedances in the structure, connecting them with transmission line will effect their predictability.

When considering the calculation method one must also consider the observable of interest, in the above cases input impedance was generally well reproduced by both schemes. This was independent of structure size however when looking at the error over all the currents the standard method performed poorly for larger cases. The standard method also performs poorly when reproducing far field patterns of large structures. If a designer was interested in the far field pattern the improved method would be a better option. The reason why it is still possible to reproduce an accurate input impedance with a large structure when using the standard method is down to the effect of elements electrically far from the observation point have. Consider a half wavelength dipole antenna and the same antenna with a small wire segment placed one wavelength away. *Figure B.20(a)* shows the input impedance of these two structures on the Smith chart, the is almost not difference in the pattern. By contrast the gain of the two structures, in *Figure B.20(b)*, much greater difference in the two curves.

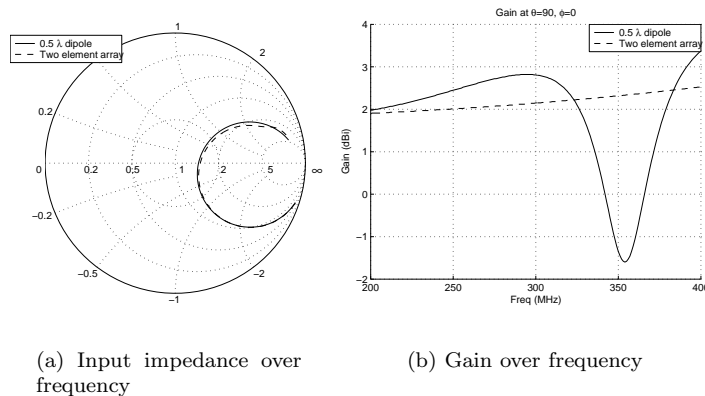


Figure B.20: Input impedance and gain over dipole and dipole with electrically distant placed element

The final aspect when considering the accuracy of the proposed method is the variation in the observable parameter. While the actual numerical error in solution is no greater in an observable with greater variation the perceived error may be. In EM design the position and magnitude of peaks and null in the observable is very important. The solution when using impedance matrix interpolation may show a small numerical error however a large offset in the placement of the peaks over frequency may result. While a flatter frequency curve with the same error would be no cause for concern. If the observable has a large amount of variance over frequency a smaller simulation range should be used. The design stage will also effect the simulation range chosen, in early stages of design greater error could be accepted if a large enough speedup in simulation time is achieved. As the design process develops designers should use smaller simulation ranges and for the greatest level of accuracy revert to the direct simulation method.

B.8 Conclusion

This appendix outlined the error analysis the impedance matrix interpolation methods implemented in the *SuperNEC* code. When using these methods to optimise MoM care must be taken in choosing the correct simulation range and sample range. The simulation range is defined as the frequency band used in the simulation extending equally on either side of the centre frequency. While the sample range is the range in MHz between the first and last sample point, as three samples are generally used in the calculation the impedance matrix fitting functions the two outer most sample points are aligned to the ends of the sample range and the second to the centre frequency. Linear sampling intervals have been used for simplification however non-linear ones could be used. The sample range and simulation range is determined by the maximum interaction distance of the two outer most segments in the structure. A form of look up table has been developed to determine the sample range for a given simulation range and maximum interaction distance. Error as a function of maximum interaction distance was shown to be constant for the improved case while it increases greatly with increasing interaction distance when applying the standard method. The effect of problem size was shown to have little effect on the overall accuracy of the problem provided the correct sample and simulation ranges were used. A confidence interval was defined as the area around the centre frequency where the mean square error in the structure currents is less than 10%, the confidence interval is generally greater in the upper frequency ranges than the lower with respect to the centre frequency. Various structures were tested using the *SuperNEC* engine and the two impedance matrix interpolation methods. Both methods perform well for electrically small structures. As the maximum interaction distance increases past a wavelength the improved method shows significantly better results, having both a lower error over the simulation range and a greater confidence interval. When simulating the LPDA antenna the error over frequency showed a few sporadic points of increased error, this is attributed to the transmission lines in the structure. However the LPDA antenna is a good candidate for impedance matrix interpolation as wide band information of the antenna's observable parameters is needed. When computing radiation patterns the standard method or direct *SuperNEC* computation should be used, the standard method was shown to not accurately reproduce far field patterns. The use of this optimisation method on UTD case should be used with caution, however with the speedup in solving the MoM equation makes it an attractive option. More research is required to apply impedance matrix interpolation for the UTD case. In general if antenna input impedance are the only observable of interest either method can be used accurately provided the correct sample and simulation range is used. Correct structure segmentation is also of great importance when using these methods the structure should be segmented at the highest frequency point of interest.

References

- [1] N. I. O’Leary. *A SuperNEC Implementation of Model Based Parameter Estimation by Interpolating the Method of Moments Impedance Matrix*. MSc(Eng) Dissertation, University of the Witwatersrand, Johannesburg, 2006. Appendix A: Theory and Method.
- [2] E. Newman. “Generation of Wide-Band Data from the Method of Moments by interpolating the Impedance Matrix.” *IEEE Transactions on Antennas and Propagation*, vol. 36, no. 12, pp. 1820–1824, DEC 1988.
- [3] J. Yeo and R. Mitta. “An Algorithm for Interpolating the Frequency Variations of Method-of-Moments Matrices Arising in the Analysis of Planar Microstrip Structures.” *IEEE Transactions on Microwave Theory and Techniques*, vol. 51, no. 3, pp. 1018–1025, MAR 2003.
- [4] Poynting Innovations. *SuperNEC Input User Reference Manual*, 2.9 ed.
- [5] J. D. Kraus. *Antennas*. McGraw-Hill, 2nd ed., 1988.
- [6] E. K. Miller. “Model-Based Parameter Estimation in Electromagnetics: Part II. Application to the EM observable.” *IEEE Antennas and Propagation Magazine*, vol. 40, no. 2, pp. 51–65, APR 1998.
- [7] G. J. Burke and A. Poggio. *Numerical Electromagnetics code (NEC) - Method of Moments*. Lawrence Livermore Laboratory, January 1981.
- [8] N. I. O’Leary. *A SuperNEC Implementation of Model Based Parameter Estimation by Interpolating the Method of Moments Impedance Matrix*. MSc(Eng) Dissertation, University of the Witwatersrand, Johannesburg, 2006. Appendix B: Efficiency Analysis.
- [9] V. P. J. Yeo, S. Köksoy and R. Mittra. “Efficient Generation of Method of Moments Matrices Using the Characteristic Function Method.” *IEEE Transactions on Antennas and Propagation*, vol. 52, no. 12, pp. 3405–3410, DEC 2004.
- [10] A. R. Clark and A. P. C. Fourie. *Antennas in Practice: EM fundamentals and antenna selection*, chap. 3, pp. 38–39. Poynting Innovations, 2001.
- [11] Poynting Innovations. *SuperNEC UTD Technical Reference Manual*, 2.9 ed.
- [12] R. Hartleb. *Optimised Ray Tracing for the SuperNEC Implementation of the Uniform Theory of Diffraction*. MSc(Eng) Dissertation, University of the Witwatersrand, Johannesburg, 2006.

Appendix C

Impedance Matrix Interpolation Efficiency Analysis

C.1 Introduction

Generation of wide band electromagnetic information is a time consuming task when using the method of moments (MoM) as the $N \times N$ impedance matrix ($[Z]$) is filled and solved at every frequency point of interest. The required time in calculating the matrix elements themselves can be reduced by approximating the elements with a simpler fitting function. This evaluation time of the fitting function is significantly less than calculating them with direct computation. Two Model- Based Parameter Estimation (MBPE) impedance matrix interpolation methods have been implemented. A standard method where the elements in the impedance matrix are approximated with the use of quadratic functions and an improved method where the frequency variant component is removed before the quadratic functions are used to approximate the function. The calculation of the fitting functions involves sampling the impedance matrix at three or more points, the coefficients are then solved. A certain number of frequency points must be of interest to achieve the break even point where the use of impedance matrix interpolation is faster than direct computation. The simulation time of both impedance matrix interpolation methods and the standard *SuperNEC* method have been analysed in terms of each of the components in there evaluation. The components are initial setup and file write time, filling the matrix and the factor and solve routine for direct computation. The MBPE method includes the time required to compute the fitting functions and then time to fill the matrix using the fitting functions. From the analysis polynomial functions are developed to approximate the simulation time in terms of the number of unknowns in the structure and the number of simulation frequencies of interest. By equating the functions it is possible to determine where the break even point is and simulation time improvements obtainable when using the impedance matrix interpolation methods. Various large structure have been simulated using each version of the code to show the time gain for real applications. Along with the large structures smaller antennas were simulated and a structure with the inclusion of a uniform geometric theory of diffraction (UTD) plate included. The simulation time of each of these examples in analysed. For the Figures, Tables and Equations in the following sections MBPE₁ refers to the standard interpolation method and MPBE₂ the improved interpolation method, for the details of the theory and implementation of these methods see [1].

This document contains analysis of the standard SuperNEC and both MBPE codes simulation time. The simulation time in analysed in terms of seconds to complete the entire simulation or a part of it.

C.2 Simulation Time

[2, 3] shows that the filling of the impedance matrix $[Z]$ is a computationally expensive task, largely due to the integration required in determining each of the matrix values. This fill time is reduced with the use of the MBPE impedance matrix interpolation methods, the method used in the impedance matrix interpolation can be found in [1]. Analysis of the simulation time for the various methods is done approximating a polynomial function with the simulation parameters [4], where number of unknowns, sample points and simulation frequencies are variables in the function. Each of the terms in the polynomial have constant coefficients which relate the equations to the simulation time of the code in seconds. Note that these coefficients will only be valid for personal computer on which the code was tested, however the code efficiency is related to the original *SuperNEC* code making it possible to determine how efficient the code is given a structure and number of simulation frequencies.

SuperNEC simulation time

The standard SuperNEC code simulation time can be analysed by the polynomial function in (C.1), where the $a_1 N^2 N_f$ term is the time to fill the MoM matrix equation, the K is the time required in initialising the simulation and writing data to the output file. Initialisation

time includes the structure setup time, initialisation of global variables and pointers, and writing initial information to the output file. This setup time is constant to all methods. Computational time required to fill and solve the matrix is of interest in the analysis of the MBPE code, specifically the matrix fill time. For more information on the matrix fill procedure and the Method of Moments see [2, 5], and specifically for SuperNEC see [3]. The number of boundary conditions varies with the number of segments connected to the source segment, thus the term a_1 is not constant for any given antenna problem. SuperNEC makes use of LU decomposition when solving the matrix [2] which is an N^3 process.

$$OC(N, N_f)_{\text{mom}} = (a_1 N^2 + a_s N^3) N_f + K \quad (\text{C.1})$$

Where:

- N = number of unknowns
- N_f = number of simulation frequencies
- a_1 = Impedance matrix fill coefficient
- a_s = Impedance matrix solve coefficient

Figure C.1 shows the time required to factor and solve in the MoM impedance matrix versus the number of unknowns in the simulation. The factor time is the time required for the LU decomposition and the solve time the time required in multiply the inverse matrix. As expected, computational time to invert the matrix is follows a cubic function.

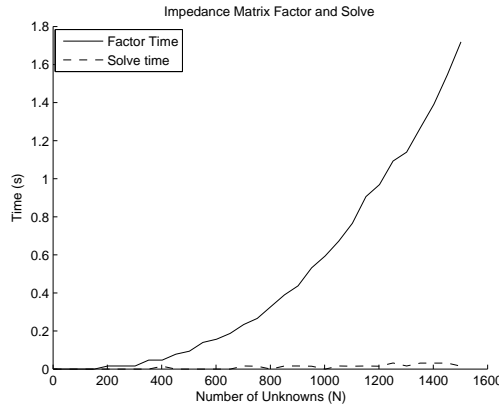


Figure C.1: MoM impedance matrix factor and solve time

MPBE₁ simulation time

Impedance matrix interpolation simulation time for can be modeled by the function in (C.2), it is noted that the coefficients a_0^s and a_1 are the same at those in (C.1). As the impedance matrix is not factored and solved only the fill time is required. Hence to obtain an improvement in simulation time the condition $a_2 \ll a_1$ must hold, where the term $a_2 N^2 N_f$ is the fill and solve time using the MBPE method. The impedance matrix elements are determined by evaluating a second order polynomial, which is computationally less complex than the standard method.

$$OC(N, N_f)_{\text{mbpe}_1} = (a_2 N^2 + a_s N^3) N_f + a_1^f N^2 N_s + a_3 N^2 + K \quad (\text{C.2})$$

Where:

- N_s = number of sample points
- a_2 = polynomial evaluation time
- a_3 = polynomial coefficients solve time

Figure C.2 shows the time to evaluate all the polynomial coefficients for an $N \times N$ matrix. It is found that it takes 8.3 Milli seconds to determine the polynomial coefficients for each of the matrix values.

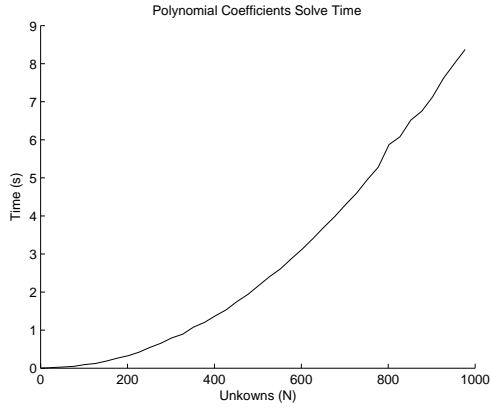


Figure C.2: Polynomial Coefficient Solve time

MPBE₂ simulation time

The second, improved, MBPE method includes the removal the dominant frequency variation term $e^{-j2\pi\lambda\vec{r}_{mn}}$. This results in an increase in simulation time when compared to the first MBPE method, as this term is removed before the polynomial coefficients are calculated. This factor is once again included after impedance matrix elements have been calculated evaluating the polynomial.

$$OC(N, N_f)_{\text{mbpe}_2} = (a_s N^3 + a_3 N^2 + a_4 N^2) N_f + a_1^f N^2 N_s + a_3 N^2 + K \quad (\text{C.3})$$

Where:

a_4 = Frequency variation evaluation time

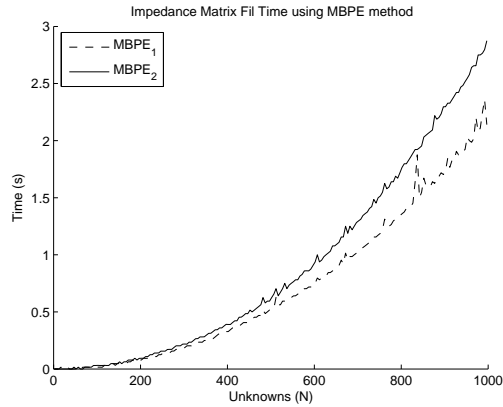


Figure C.3: Impedance matrix fill time via polynomial interpolation

C.3 Results

Simulation time coefficients

Approximate values have been obtained for the simulation time coefficients by simulating with increasing problem size, polynomial approximations where techniques were applied to the test results to obtain the approximate coefficient values. These values are shown in Table C.1. All the simulation were performed on a Pentium 4 3.8 GHz personal computer

with 2GB RAM, running Windows XP. The simulation time will naturally differ on other systems.

Table C.1: Simulation time equation coefficients

| Coefficient | Coefficient Name | Value |
|-------------|-------------------------------------|-------------|
| a_s | Matrix Solve time | $6.2E - 10$ |
| a_1 | SuperNEC fill time | $7E - 6$ |
| a_2 | Polynomial coefficient solve time | $8,9E - 6$ |
| a_3 | Polynomial evaluation time | $5,4E - 6$ |
| a_4 | Frequency variation evaluation time | $0,9E - 6$ |

In order to achieve an increase in performance a certain number of frequency points must be of interest, this is to overcome the initial time in sampling the matrix and solving the polynomial coefficients. Solving the requirement of simulation time decrease, $OC_{mbpe_1} - OC_{mom} \leq 0$, it is found that 17 frequency points are required. Using the same method for the second MBPE method, 38 frequency points are required. For both these cases three impedance matrix samples are taken. Figures C.4(a) and C.4(b) shows the simulation time gain improvement obtained when using the impedance matrix interpolation schemes as a function number of unknowns and simulation frequencies.

Yagi antenna

The Yagi-Uda structure in Figure C.3 was simulated at 100 frequency points ranging from 200MHz to 700MHz at 5MHz intervals. To increase the complexity of the structure one wire grid was placed below the structure and another behind it. The structure was segmented to a frequency of 700MHz, resulting in 1327 segments in the structure. Hence the problem size $N = 1327$, with a 1327×1327 impedance matrix.

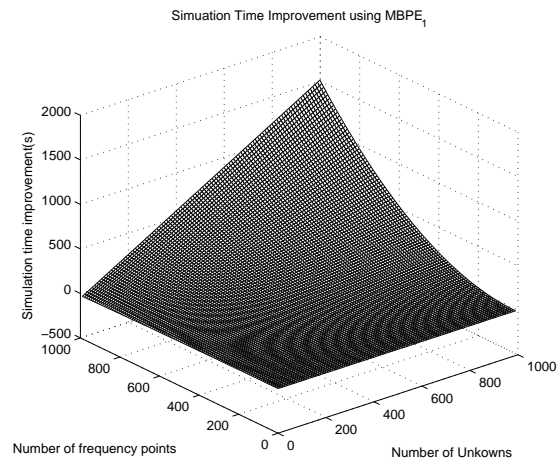
Table C.2 shows the simulation, fill and solve times are more efficient when using the MBPE methods. The matrix fill time is twice as fast as using direct MoM, however due to the time required to factor and solve the matrix is the same for both case, the over all simulation time reduction is not as great.

Table C.2: Yagi - Uda structure simulation time

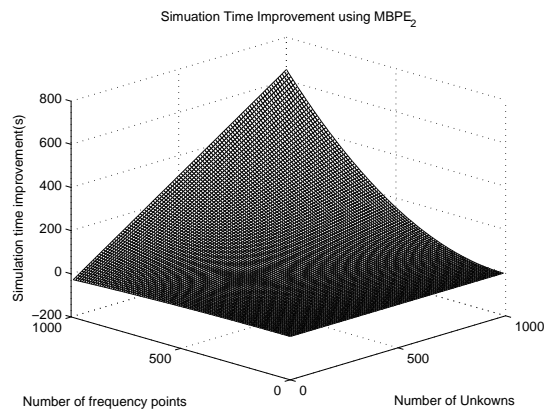
| Method | Simulation time (sec) | Fill Time (sec) | Solve time (sec) |
|-------------------------|-----------------------|-----------------|------------------|
| <i>SuperNEC</i> | 2513 | 26,87 | 1,25 |
| <i>MBPE₁</i> | 1205 | 9,67 | " |
| <i>MBPE₂</i> | 1278 | 10,2 | " |

Patch antenna

The code was tested using a patch antenna, a structure with greater number of connections at the segment nodes. Hence there are more boundary conditions for each segments and the filling procedure for the direct MoM is slower than if all the segments in the structure where unconnected. The antenna was segmented such that there where 4170 unknowns in the simulation, 80 frequency points where used, ranging from 460MHz to 540MHz in 1MHz intervals. As the SuperNEC code currently only operates in free space [6], no dielectric was used between the patch and ground plane. Table C.3 compares the results obtained using the different codes, once again the first MBPE method is faster than the second method, however both are significantly faster than the direct method. The fill time using MBPE is more than twice as fast and the overall simulation time is 33% of the overall SuperNEC simulation time.



(a) MBPE₁



(b) MBPE₂

Figure C.4: Mesh plot showing simulation time reduction (in seconds) for the impedance matrix interpolation schemes versus number of unknowns and simulation frequencies

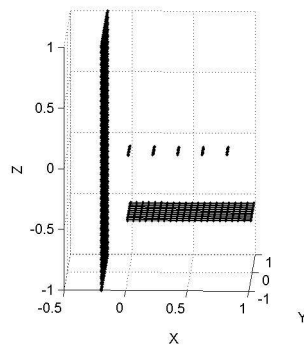


Figure C.5: 5 Element Yagi-Uda Antenna with wire grids

| Method | Simulation time (sec) | Fill Time (sec) | Solve time (sec) |
|-------------------|-----------------------|-----------------|------------------|
| <i>SuperNEC</i> | 17031 | 255,625 | 30,656 |
| MBPE ₁ | 11312 | 97,547 | " |
| MBPE ₂ | 12772 | 114,313 | " |

Simulation time from examples in [7]

The simulation time of the structures tested in the error analysis section [7] will be discussed. The antennas simulated where a half wavelength dipole, a five element yagi antenna, an log periodic dipole array (LPDA), a horn antenna and the previous yagi antenna with uniform theory of diffraction (UTD) plate included. The centre frequency of $500MHz$ was used for all the antenna except for the horn where $300MHz$ was used. The simulation range was selected by the method shown in [7] which specifies the simulation range as a function of the interaction distance of the two further most segments in the structure. This method is shown to work well for maximum interaction distances greater than a wavelength. The sample range was also chosen using the method proposed however holds no relevance in the analysis of the simulation time.

The method used to determine the simulation time increase (%) is

$$\text{Simulation time increase(\%)} = \frac{OC_{\text{mom}} - OC_{\text{mpbe}}}{OC_{\text{mom}}} \times 100 \quad (\text{C.4})$$

Table C.4: Table showing simulation time for test cases with standard interpolation (MBPE₁)

| | No Segments | No Freq points | Increase in Simulation time (%) |
|--------|-------------|----------------|---------------------------------|
| Dipole | 15 | 255 | 36 |
| Yagi | 50 | 231 | 53 |
| LPDA | 221 | 99 | 41 |
| UTD | 50 | 231 | 2700 |
| Horn | 1289 | 21 | 40 |

Table C.5: Table showing simulation time for test cases with improved interpolation (MBPE₂)

| | No Segments | No Freq points | Increase in Simulation time (%) |
|--------|-------------|----------------|---------------------------------|
| Dipole | 15 | 339 | 34 |
| Yagi | 50 | 307 | 51 |
| LPDA | 221 | 133 | 39 |
| UTD | 50 | 307 | 2700 |
| Horn | 1289 | 21 | 36 |

The timing equations are shown to have a similar trend as the real results however the values are not exact. This is attributed to the fact that the coefficients in the equations where determined with the use of curve fitting methods and where not exact reproductions of the parameters.

The result in *Tables C.4* and *C.5* shows a good increase in simulation time can be made with by using the impedance matrix interpolation methods. Gains in simulation time are made with smaller structures, the method becomes a usefull one when dealing with many unknowns (more than 100) in the structures and simulation over a wide frequency band with small frequency steps. As the problem size becomes too great however the amount of memory needed in the storage of the samples and coefficients becomes great (more than 1GB), this is less of a problem as many personal computers have over a 1GB of RAM and and can easily have up to 4GB.

C.4 Conclusion

The implementation impedance matrix interpolation schemes was shown to reduce the simulation time in solving the MoM equation. This is done by reducing the computational time in filling the impedance matrix by interpolation each of the elements with a simpler function which can be evaluated faster than using direct computation. The increase in speed depends largely on the size of the structure under test and the number of simulation frequency points of interest. Mathematical functions have been developed to relate the simulation time to the parameters in the frequency domain simulation being number of unknowns and simulation points. In determining the fitting model extra time is used in sampling the impedance matrix by direct computation and solving the fitting model coefficients. A break even point is where the use of the MBPE method is faster than using the direct *SuperNEC* method, this break even point is dependent of the number of unknowns and simulation points. From the theoretical models the break even points was found to only depend on the number of simulation points being 17 for the standard method and 38 in the improved case. When applied to real cases less simulation points were needed for larger structures, as was the case with the horn antenna where 21 simulation points resulted in a 40% improvement in simulation time. In general the improvement in simulation time for the tested cases was found to be around 40%. This is because the number of frequency range which the MBPE method can be used accurately decreasing with increasing interaction distance in the structure, which generally means an increase in problem size. While speed up is made with structures with a small number of unknowns it is only with the larger structures over a wider frequency band where the method becomes useful. When the problem size is small simulation time is so fast (in terms of seconds) that the speed up is not really worth the loss in accuracy. By contrast when the problem size increases past 100 unknowns the reduction in simulation time is significant as simulations can take many minutes and even hours. If a designer was doing multiple simulation over a wide frequency range in order to optimise a design the reduction in time would become significant. Electrically large structures, such as horn antennas and those requiring wide band simulation data, such as LPDAs, are best suited to the use of impedance matrix interpolation as a method to reduce simulation time. Smaller antennas and those which require narrow band information should be simulated using the standard *SuperNEC* engine. *SuperNEC* does not have the functionality to simulate dielectrics and substrates other than air. When impedance matrix interpolation is applied to MoM field solver with the ability to solve problems of this nature it is shown to greatly reduce the simulation time [8, 9]. The method was applied to the UTD case with a great reduction in simulation time, over 29 times faster. The application to the UTD case however showed poor level accuracy in the MoM solution and more research is required to apply the method to this case.

References

- [1] N. I. O’Leary. *A SuperNEC Implementation of Model Based Parameter Estimation by Interpolating the Method of Moments Impedance Matrix*. MSc(Eng) Dissertation, University of the Witwatersrand, Johannesburg, 2006. Appendix A: Theory and Method.
- [2] G. J. Burke and A. Poggio. *Numerical Electromagnetics code (NEC) - Method of Moments*. Lawrence Livermore Laboratory, January 1981.
- [3] D. Nitch. *A serial and parallel design of NEC2 to demonstrate the advantages of the object-oriented paradigm in comparison with the procedural paradigm*. Ph.D. thesis, School of Electrical Engineering, University of the Witwatersrand, 1992.
- [4] E. K. Miller and G. J. Burke. “An overview of some selected topics in computational electromagnetics: Present status and future directions.” In *SAIEE Joint Symposium on Antennas and Propagation and Microwave Theory and Techniques*, pp. 1–10. August 1986.
- [5] R. F. Harrington. *Field Computations by Moment Methods*. New York: McMillan, 1968.
- [6] Poynting Innovations. *SuperNEC Getting started User Manual*, 2.3 ed.
- [7] N. I. O’Leary. *A SuperNEC Implementation of Model Based Parameter Estimation by Interpolating the Method of Moments Impedance Matrix*. MSc(Eng) Dissertation, University of the Witwatersrand, Johannesburg, 2006. Appendix C: Error Analysis.
- [8] J. Yeo and R. Mittra. “An Algorithm for Interpolating the Frequency Variations of Method-of-Moments Matrices Arising in the Analysis of Planar Microstrip Structures.” *IEEE Transactions on Microwave Theory and Techniques*, vol. 51, no. 3, pp. 1018–1025, MAR 2003.
- [9] V. P. J. Yeo, S. Köksoy and R. Mittra. “Efficient Generation of Method of Moments Matrices Using the Characteristic Function Method.” *IEEE Transactions on Antennas and Propagation*, vol. 52, no. 12, pp. 3405–3410, DEC 2004.

Appendix D

Radiation Pattern Interpolation

D.1 Introduction

Computation of the far field pattern or radiation pattern is a computationally expensive task, as the far field is to be calculated at each of the spacial and frequency points of interest. To generate a three dimensional far field information in one degree increments: 64,800 values must be calculated. This is done at every frequency point of interest. Another issue with generating radiation patterns using this method is storage, three dimensional radiation pattern information over a wide frequency band would result in a output file of many megabytes in size. If one could use model-based parameter estimation (MBPE) to generate a fitting model to approximate the radiation pattern computational time and storage could be reduced significantly. Generating a fitting model for an EM observable parameter such as radiation pattern requires the use of a fitting function, such as a rational function, able to reproduce the peaks and nulls encountered in the parameter [1]. Radiation pattern MBPE was implemented by Werner in [2] to interpolate antenna radiation patterns spatially and over frequency. The method uses a rational function to approximate the radiation pattern. This technique was implemented in Matlab using radiation generated by *SuperNEC*, however produced poor results. A single rational function in a single dimension was used to approximate firstly the gain over frequency and later the radiation pattern spatially.

D.2 MoM far field calculation

[3] shows that the radiated far field at an arbitrary observation point from an antenna modelled with thin wires in NEC can be calculated by:

$$\vec{E}(\vec{r}_o) = \frac{jkn}{4\pi} \frac{e^{-jkr_o}}{r_o} \int_L \left[\left(\hat{k} \cdot \vec{I}(s) \right) \hat{k} - \vec{I}(s) \right] e^{j\vec{k} \cdot \vec{r}} ds \quad (D.1)$$

Where \vec{r}_o is the observation point, $k = 2\pi/\lambda$, $\vec{k} = \vec{r}_o/|\vec{r}_o|$ and $\hat{k} = k\vec{k}$. The integral in the equation is evaluated in closed form each of the segments in the structure. As the structure has been discretised the integral is reduced to the sum over all the segments. The current $I(s)$ is the solution of the MoM procedure outlined in [3, 4], thus it follows that the sum used to solve the above integral will be N in size, where N number of segments, or unknowns, in the structure.

The antenna gain in spherical coordinates (θ, ϕ) is determined by:

$$G_p(\theta, \phi) = 4\pi \frac{P(\theta, \phi)}{P_{in}} \quad (D.2)$$

where P_{in} is the total antenna power at the source calculated by:

$$P_{in} = 0.5\Re(VI^*) \quad (D.3)$$

And using (D.1) $P(\theta, \phi)$ is determined by:

$$P(\theta, \phi) = \frac{|r_o|^2}{2\eta} \left(\vec{E} \cdot \vec{E}^* \right) \quad (D.4)$$

From this formulation it is clear that wideband far field information is generated at great computational cost. The operation count for determining a far field field pattern at N_f frequency points, N_θ θ and N_ϕ ϕ points for a N segment large structure is:

$$OC = NN_\theta N_\phi N_f \quad (D.5)$$

A similar amount of storage is required to store the far field information. A model-based fitting model solution would be an obvious approach to reduce both the computational cost and storage needed for the process. The fitting model could be used to replace the data set entirely and be used to plot far field information and find features of interest such as peaks and null with the use of standard numerical methods.

D.2.1 Rational function overview

A rational function is a n^{th} upon m^{th} order polynomial, also known as a ratio of polynomials. Rational functions are useful fitting models as they can reproduce nulls and peaks encountered in many electromagnetic observables such as far electric field spatially and over frequency. Determining rational function coefficients is done with aid of the Padé approximation and shown below.

$$f(x) = \frac{\sum_{i=0}^n a_i x^i}{\sum_{j=0}^m b_j x^j} = \frac{a_n x^n + a_{n-1} x^{n-1} + \dots + a_1 x + a_0}{b_m x^m + b_{m-1} x^{m-1} + \dots + b_1 x + b_0} \quad (D.6)$$

$$(D.7)$$

To determine coefficients the function $a(x)$ is multiplied by an arbitrary constant resulting in $b_0 = 1$, by multiplying (D.7) out we obtain :

$$0 = a_0 + a_1 x + \dots + a_n x^n - 1 - b_1 x f(x) - \dots - b_m x^m f(x) \quad (D.8)$$

The resulting coefficients are solved by sampling the function $f(x)$ at $m + n + 1$ points. The resulting linear system is solved in matrix form.

D.2.2 Implementation

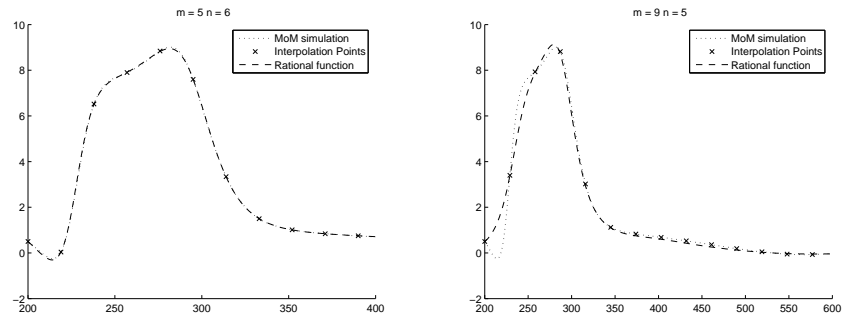
Rational functions of various orders were used to approximate antenna gain over frequency for wire antenna structures. p antenna gain values were sampled at constant Δf interval and a rational function of $\frac{m}{n}$ was calculated with the use of Matlab. The resulting rational function model was compared to original gain information generated by *SuperNEC*. A “best-fit” procedure was used to determine the most accurate values for m and n .

When the correct fitting order is used very accurate results can be obtained, *Figure D.1(a)* shows the gain pattern of a yagi-uda type antenna over the 200 – 400 MHz frequency range. Here a $\frac{5}{6}$ fitting order was used, however *Figure D.1(b)* shows the gain of the same antenna over a wider frequency band. In this case the best possible approximation uses a $\frac{9}{5}$ fitting order. It is important to note that the two fitting functions, while both are applied to the same antenna, have significantly different rational function order.

If the incorrect fitting order is used entirely high inaccurate results are obtained, *Figure D.2* is the same curve as in *Figure D.1(a)* with a different order rational function used to approximate the gain. This gain pattern is not very featured in terms of peaks and null in the pattern over frequency and it is still difficult to predict the fitting order. Note the linear sampling was used, hence the sample points are equally spaced over the sample range, if an improved sampling method was employed it may be able to produce better results with any given fitting order.

Spacial interpolation of radiation pattern was also done. Simulations over the theta (θ) range were done while keeping phi (ϕ) at zero. As with the previous examples, rational function approximations were used with varying m and n orders to find the best approximation. *Figure D.3* shows the spacial far field pattern from the Yagi antenna in the examples above, the dotted line shows the rational function approximation. Once again if the correct rational function orders are chosen an accurate approximation can be generated using this form of fitting model.

The difficulty in implementing MBPE on radiation patterns is to develop a generic solution for any structure or antenna case. In the examples outlined above the complexity of the radiation pattern, in the frequency and spacial domain, was low. With increasing the number



(a) 200 – 400MHz

(b) 200 – 600MHz

Figure D.1: Gain over frequency of a Yagi antenna with a Padé rational function fitting model

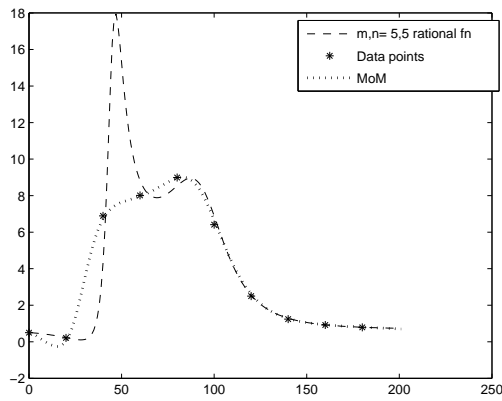


Figure D.2: Yagi gain pattern as in *Figure D.1(a)* with and incorrect rational function order fitting model

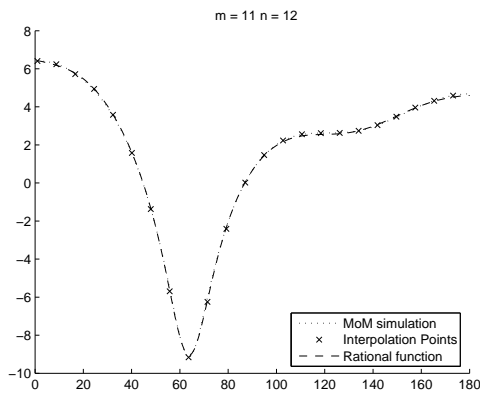


Figure D.3: Yagi Radiation pattern $90^\circ \leq \theta \leq 270^\circ$ with rational function interpolation

of peaks and nulls in the farfield pattern this method of radiation pattern interpolation becomes more complex. Position of nulls in frequency or specially is generally a large consideration in antenna design [5], if a fitting model is unable to predict there position it would be considered impractical. Werner in [6] further improved his approach with the use of windowed functions to approximate the radiation pattern. This method used a number of rational function of constant order to approximate sections of the radiation spatially and pattern over frequency. This method showed improved results however with simple cases. One possible use of this techniques would be to reduce the amount of storage needed for three dimensional far field pattern. If a fitting model was calculated and stored instead of the numerical value at each of the points of interest a large saving in storage could be achieved. An accurate fitting model could be found as the full data set is available to calculate the fitting model. Position a frequency of peaks and nulls could be precisely found, hence the order of the rational function or transfer function would known. This method would not reduce the required computational time to calculate far field patterns much, however fewever points could be used than are used to develop the full numerical solution.

D.3 Conclusion

Radiation patterns, spatially and over frequency, generated by *SuperNEC* was approximated with Padé rational function. Given the correct rational function order the method could reproduce the curve accurately, however an incorrect order resulted in a highly inaccurate results. Since it is not obvious as to the fitting order of the rational function this method is difficult to implement as to generic structures. Storage of the fitting model instead of the numerical data would drastically decrease the amount of storage required for radiation patterns. The far field however would still need to be calculated from the direct method of moments method and the fitting model calculated of an extensive data set.

References

- [1] E. K. Miller. “Model-Based Parameter Estimation in Electromagnetics: Part II. Application to the EM observable.” *IEEE Antennas and Propagation Magazine*, vol. 40, no. 2, pp. 51–65, APR 1998.
- [2] D. H. Werner and R. J. Allard. “The simultaneous interpolation of antenna radiation patterns in both the spatial and frequency domains using Model-Based Parameter Estimation.” *IEEE Transactions on Antennas and Propagation*, vol. 48, no. 3, pp. 383–392, MAR 2000.
- [3] G. J. Burke and A. Poggio. *Numerical Electromagnetics code (NEC) - Method of Moments*. Lawrence Livermore Laboratory, January 1981.
- [4] N. I. O’Leary. *A SuperNEC Implementation of Model Based Parameter Estimation by Interpolating the Method of Moments Impedance Matrix*. MSc(Eng) Dissertation, University of the Witwatersrand, Johannesburg, 2006. Appendix A: Theory and Method.
- [5] J. D. Kraus. *Antennas*. McGraw-Hill, 2nd ed., 1988.
- [6] D. H. Werner and R. J. Allard. “The antenna Model-Based Parameter Estimation radiation patterns Using Windowed Interpolation and Spherical Harmonics.” *IEEE Transactions on Antennas and Propagation*, vol. 51, no. 8, pp. 1891–1905, AUG 2003.